Supporting information

The role of the side chain on the performance of n-type conjugated polymers in aqueous electrolytes

Alexander Giovannitti[1,2*], Iuliana P. Maria[1], David Hanifi[3], Mary J. Donahue[4], Daniel Bryant[5], Katrina J. Barth[6], Beatrice E. Makdah[6], Achilleas Savva[7], Davide Moia[2], Matyáš Zetek[2], Piers R.F. Barnes[2], Obadiah G. Reid [10,11], Sahika Inal[7], Garry Rumbles[9,10,11], George G. Malliaras[12], Jenny Nelson[2], Jonathan Rivnay[6,8,*] and Iain McCulloch[1,5]

[1] Department of Chemistry, Imperial College London, London SW7 2AZ, United Kingdom.

[2] Department of Physics and Centre for Plastic Electronics, Imperial College London, London SW7 2AZ, United Kingdom.

[3] Department of Chemistry, Stanford University, Stanford, California 94305, United States

[4] Department of Bioelectronics, École Nationale Supérieure des Mines, CMP-EMSE, MOC Gardanne, 13541, France.

[5] Physical Sciences and Engineering Division, KAUST Solar Center (KSC), King Abdullah University of Science and Technology (KAUST), KSC Thuwal 23955-6900, Saudi Arabia

[6] Department of biomedical Engineering, Northwestern University, 2145 Sheridan Road, Evanston, IL 60208, USA

[7] Biological and Environmental Science and Engineering, King Abdullah University of Science and Technology (KAUST), Thuwal 23955-6900, Kingdom of Saudi Arabia.

[8] Simpson Querrey Institute for BioNanotechnology, Northwestern University, Chicago, IL, 60611, USA

[9] Department of Chemistry and Biochemistry, University of Colorado at Boulder, Boulder, CO 80309, USA.

[10] Renewable and Sustainable Energy Institute, University of Colorado at Boulder, Boulder, CO 80309, USA.

[11] National Renewable Energy Laboratory, Chemistry and Nanoscience Center, 15013 Denver West Parkway, Golden, CO 80401

[12] Electrical Engineering Division, University of Cambridge, 9 JJ Thomson Ave, Cambridge CB3 0FA, United Kingdom

Contents

1. Methods:

Column chromatography was performed on silica gel from VWR Scientific, using the indicated solvents. Microwave experiments were carried out in a Biotage Initiator V 2.3. ^{1}H and ^{13}C NMR spectra were recorded on a Bruker AV-400 spectrometer at 298 K and are reported in ppm relative to TMS. UV-Vis absorption spectra were recorded on UV-1601 (λ_{max} 1100 nm) UV-VIS Shimadzu UV-Vis spectrometers. MALDI TOF spectrometry was carried out in positive reflection mode on a Micromass MALDImxTOF with trans-2-[3-(4-tert-Butylphenyl)-2-methyl-2-propenylidene]-malononitrile (DCTB) as the matrix. Thermogravimetric analysis (TGA) analysis was carried out on a Mettler Toledo TGA system, heating from 30.0°C to 105.0 °C, (34.99 K/min), keeping the temperature at 105.0 °C for 10.00 min and heating from 105.0 to 800.0 °C, 10.00 K/min under nitrogen flow (50ml/min). Differential scanning calorimetry (DSC) was carried out on a TA Instruments DSC Q20 with a heating rate of 10°C/min, heating from -30 to- 330 °C to avoid decomposition of the copolymers. Contact angle were measured on a Kruss DSA 100 Goniometer with DI water. The thickness of the films prepared by spin or drop cast were measured with a profilometer (Bruker DektakXT). Thin films of the copolymers were prepared by spin coating where the copolymers were dissolved in chloroform by heating the solutions to 50 °C for 30 mins (5 mg/mL (OECT, EIS, CV, GIWAXS, UV-Vis measurements) or 10 mg/mL (OFET, and QCM measurements)).

Additional experimental methods

Photothermal Deflection Spectroscopy (PDS)

Measurements were performed on a home-built set-up described by Vandewal *et al.* .[1] The measurements were carried out by using a mechanically chopped (3.333Hz) monochromatic light source using both a 100 W halogen pump lamp with 5 nm spectral resolution focused onto the sample. Degassed and filtered perflourohexane (C6F14, 3M Flourinert FC-72) was used as the deflection medium. The films were aligned with maximal transverse overlap between the pump beam. Thin films were prepared similarly *vida supra* onto on quartz substrates with less than 1nm RMS roughness. The samples were prepared, stored and transferred in a nitrogen environment with < 0.1ppm of oxygen.

QCM-D measurements:

QCM-D measurements were performed by using a Q-sense analyzer (QE401, Biolin Scientific). First, we recorded the QCM response of the bare Au sensors (QX-338 Ti-Au QCM) in air, followed by the injection of 0.1 M aqueous NaCl solution. This resulted in a large frequency and dissipation shifts, due to the difference in density between the two media, which must be excluded from the swelling percentage calculation. The measurements were then stopped, the sensors was removed and polymer layers were spun cast on the same sensor. We compared the absolute frequency difference between the bare Au sensor and the Au/Polymer coated sensor, both in air and in NaCl solution, by using the function “stitched data” of Q-soft software. This function compares the selected datasets based on the raw frequencies measured and excludes the effect of the different densities between the two mediums. Thus, the difference of the frequency of the stitched data is directly analogous to the thickness of the polymer in both media, which is calculated by using the Sauerbrey equation.

2D-Grazing Incidence Wide Angle X-ray Scattering (GIWAXS)

X-ray scattering was conducted at the Stanford Synchrotron Radiation Lightsource (SSRL) at beamline 11-3 (with a MAR225 image-plate CCD with 73.242µm x73.242µm pixel area). Incident photon energy was 12.732 keV (0.973Å) with ~10^9 photon flux. He (g) environments for all measurements were used to minimize air scatter and beam damage to the sample. The 2D grazing-incidence sample-detector distance was 311.74 mm calibrated with a polycrystalline lanthanide hexaboride (LaB_6) standard at a 3.0^o degree angle with respect to the critical angle of the calibrant. For grazing-incidence geometries, the incidence angle was set below the critical angle, to a grazing incidence of 0.1^o which is above the critical angle the underlying native oxide substrate. The data was processed using a combination of both Nika 2D data reduction[2] and homebuilt WxDiff Software. The terms q_{xy} and q_z denote the component of scattering vector in-plane and out-of-plane with the substrate, respectively. Data from 2D grazing-incidence measurements were corrected for the geometric distortion introduced by a flat, plate detector and processed for subsequent analysis with the software WxDiff and GIWAXSTool for Igor.[3] All films were prepared on native oxide silicon substrates and measured as prepared *vida supra*.

2. Synthesis

2.1. Monomer synthesis g7-NDI-Br_2

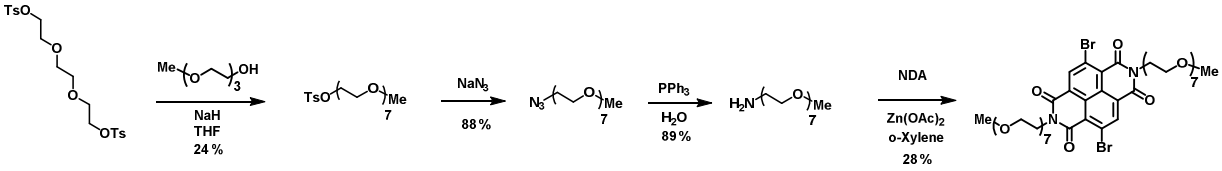

Figure S1: Overview of the synthesis of **g7-NDI-Br_2**.

2.1.1. Azide-glycol

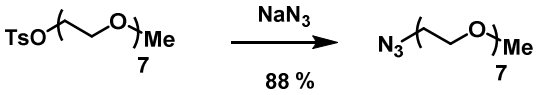

A protocol by Svedhem and co-workers was used and slightly modified.[4] A 100 mL two neck RBF was dried and purged with argon. 2,5,8,11,14,17,20-heptaoxadocosan-22-yl 4-methylbenzenesulfonate (3.26 g, 6.49 mmol) was dissolved in 15 mL of DMF. Sodium azide (0.64 g, 9.72 mmol) was added and the reaction mixture was heated to 105 °C for 2 h. After full conversion (monitored by TLC), the solvent was removed under reduced pressure and the obtained oil was purified by flash column chromatography on silica gel with ethyl acetate and methanol as the eluent in a ratio of 10 : 1. The solvents were removed under reduced pressure and the oil was dried under high vacuum for 16 h. 2.08 g of a colorless oil was obtained with a yield of 88 %.

^{1}H NMR (400 MHz, $CDCl_3$) δ: 3.68 – 3.62 (m, 24H), 3.55 – 3.52 (m, 2H), 3.39 – 3.88 (m, 2H), 3.37 (s, 3H) ppm. ^{13}C NMR (100 MHz, $CDCl_3$) δ: 72.0, 70.8 – 70.6 (multiple signals), 70.1, 59.1, 50.8 ppm. HRMS (ES-ToF): 366.2252 [MH^+] (calc. 366.2240, $C_{15}H_{32}N_3O_7$).

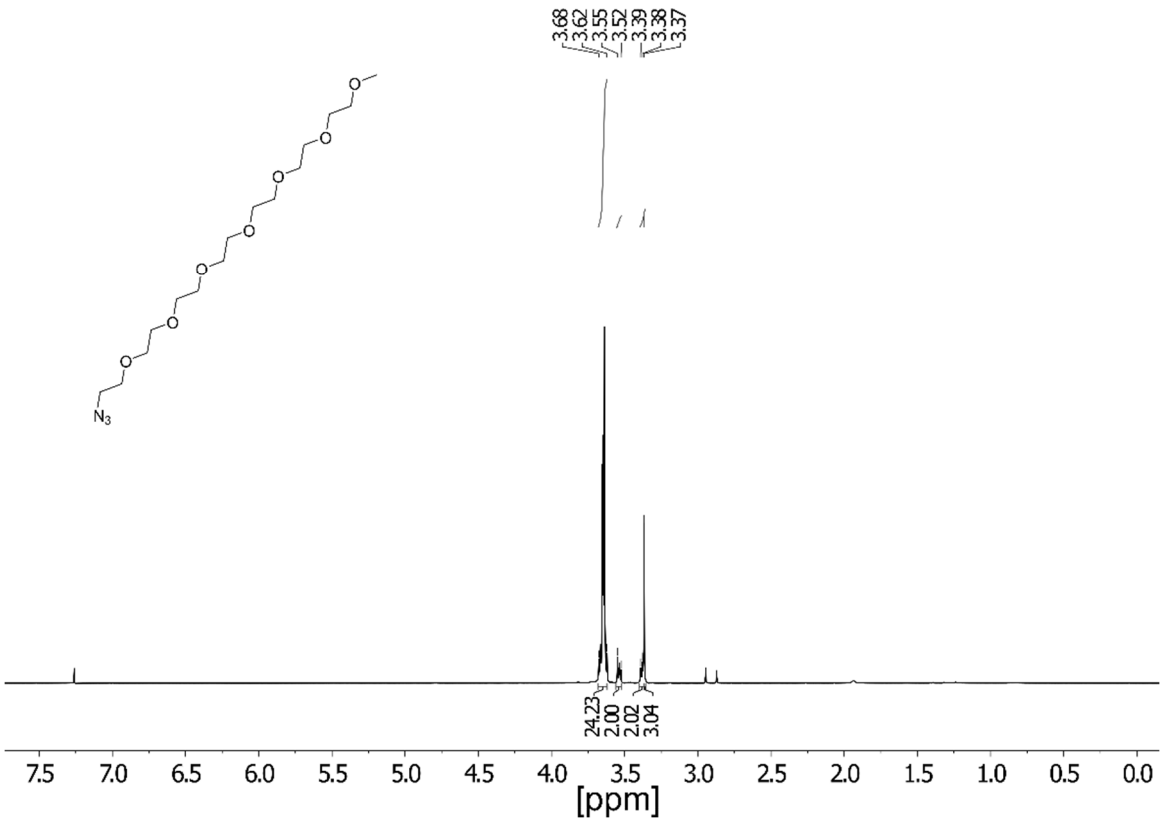

Figure S2: ^{1}H NMR spectrum of 22-azido-2,5,8,11,14,17,20-heptaoxadocosane in $CDCl_3$.

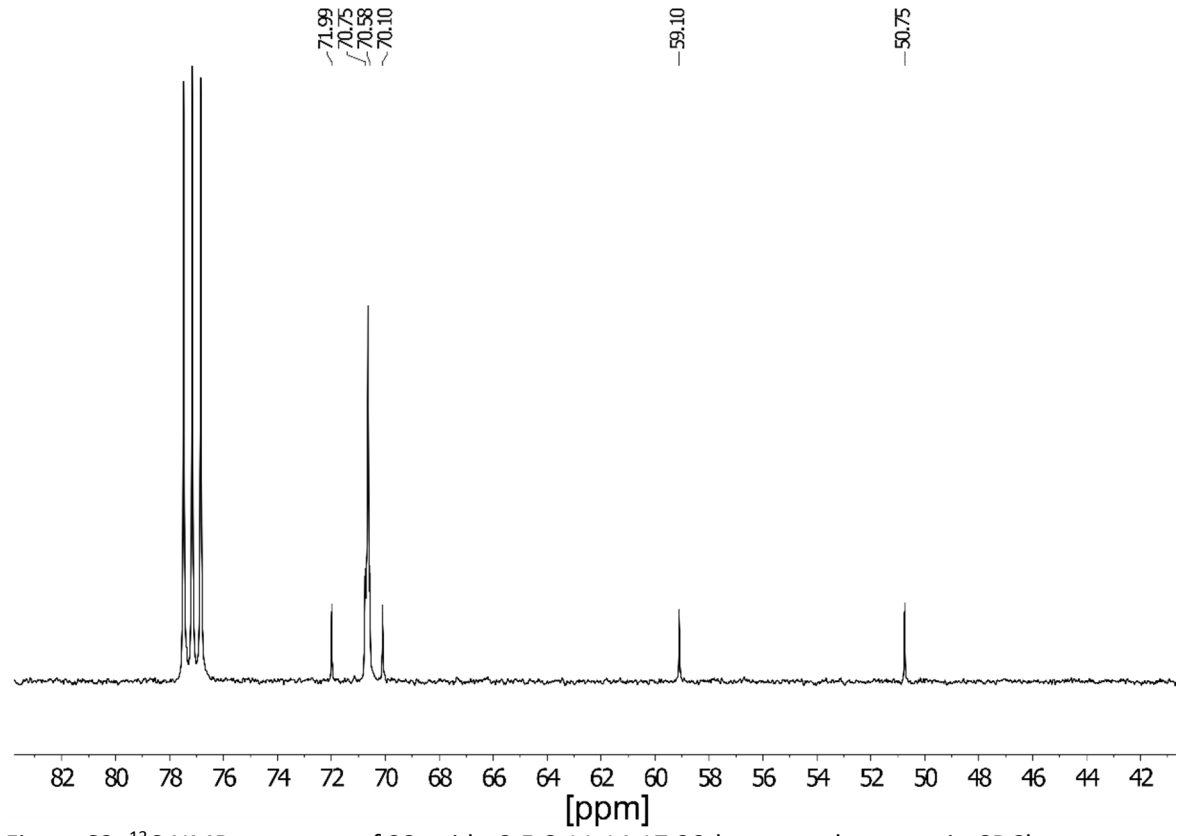

Figure S3: ^{13}C NMR spectrum of 22-azido-2,5,8,11,14,17,20-heptaoxadocosane in $CDCl_3$.

2.1.2. Amino-glycol

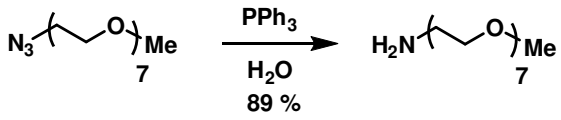

A protocol by Svedhem and co-workers was used and slightly modified.[4] A 100 mL two neck RBF was dried and purged with argon. 22-azido-2,5,8,11,14,17,20-heptaoxadocosane (2.08, 5.69 mmol, 1.0 eq.) was dissolved in 30 mL of anhydrous THF. The reaction mixture was cooled to 0 °C and triphenyl phosphine (2.24 g, 8.54 mmol, 1.5 eq.) was added in small portions and the reaction mixture was allowed to heat up to room temperature. After stirring for 8 h, the reaction was heated to 50 °C for 1 h. The reaction mixture was cooled to room temperature, quenched with 0.2 mL of water and stirred for 16 h at room temperature. After full conversion, 100 mL of DI water was added and the aqueous phase was extracted with diethyl ether to remove side products. The water was removed under reduced pressure and the product was dried at 60 °C under high vacuum for 16 h. 1.72 g of a colorless oil was obtained with a yield of 89 % (5.06 mmol).

^{1}H NMR (400 MHz, $CDCl_3$) δ: 3.84 – 3.62 (m, 24H), 3.54 – 3.52 (m, 2H), 3.50 – 3.48 (d, *J* = 10.5 Hz, 2H), 3.36 (s, 3 H), 2.86 – 2.83 (d, *J* = 10.5 Hz, 2H) ppm. ^{13}C NMR (100 MHz, $CDCl_3$) δ: 73.6, 72.1, 70.7 – 70.6 (multiple signals), 70.4, 59.2, 41.9 ppm. HRMS (ES-ToF): 340.2347 [MH^+] (calc. 340.2335).

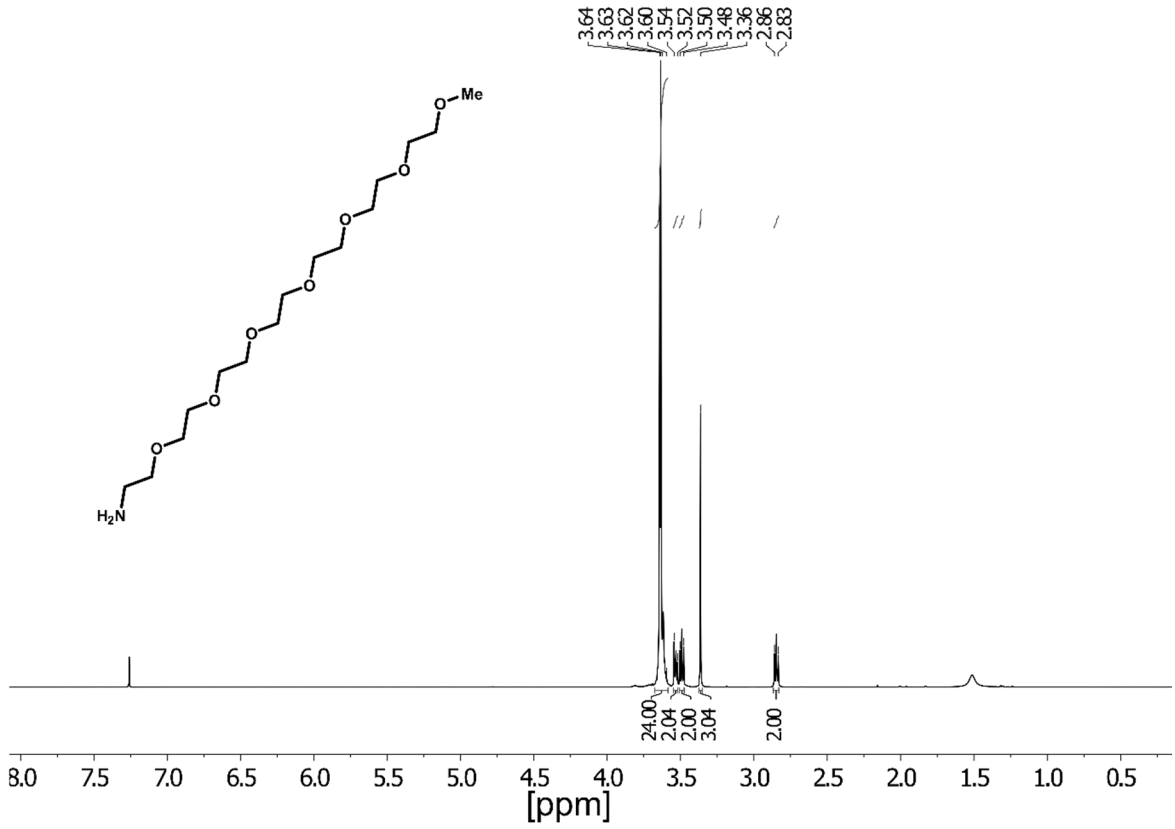

Figure S4: ^{1}H NMR of 2,5,8,11,14,17,20-heptaoxadocosan-22-amine measured in $CDCl_3$.

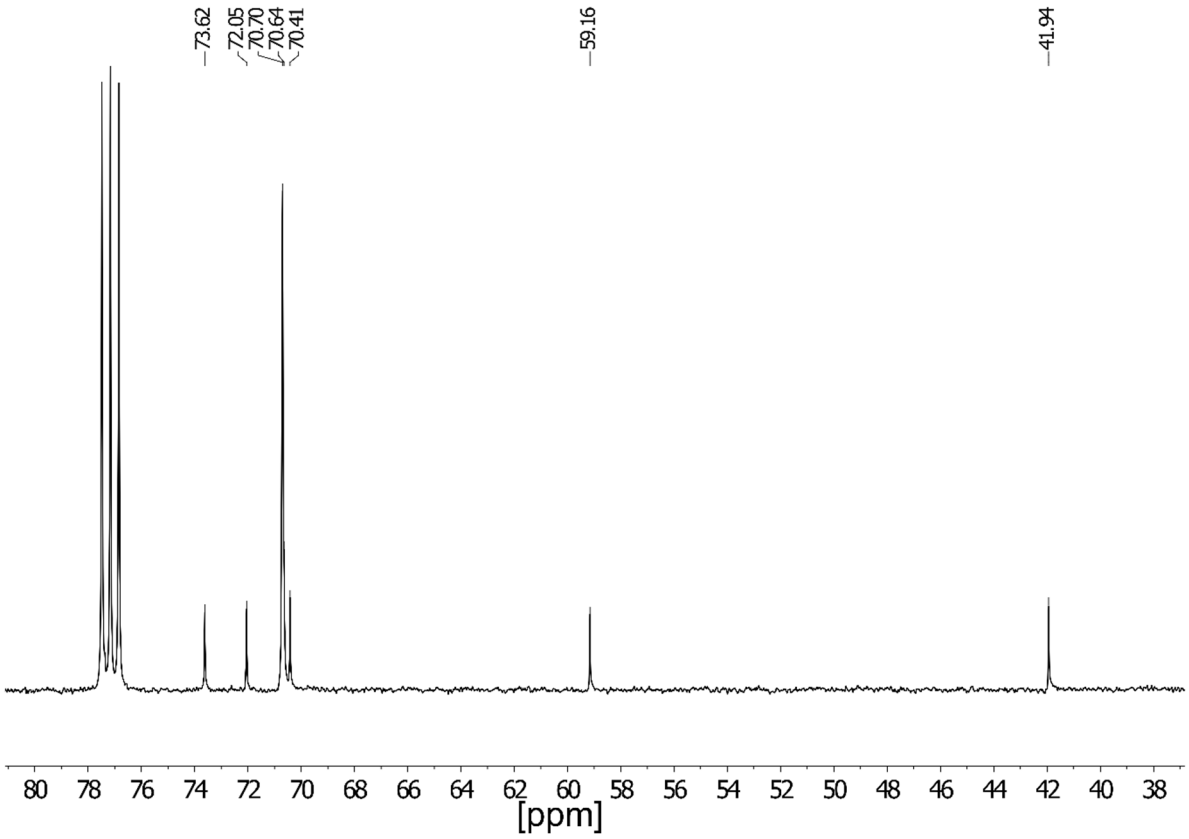

Figure S5: ^{13}C NMR of 2,5,8,11,14,17,20-heptaoxadocosan-22-amine measured in $CDCl_3$

2.1.3. g7-NDI-Br_2

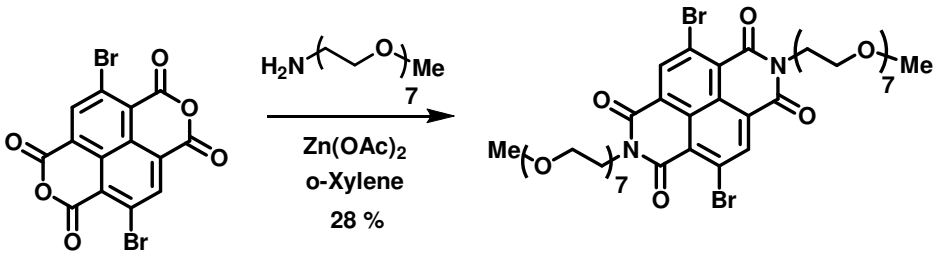

A 100 mL two neck RBF was dried and purged with argon. 2,5,8,11,14,17,20-heptaoxadocosan-22-amine (990 mg, 2.91 mmol), anhydrous zinc acetate (535 mg, 2.91 mmol) and 2,6-dibromonaphthalene-1,4,5,8-tetracarboxylic dianhydride (620 mg, 1.45 mmol) were dissolved in 50 mL of anhydrous xylene. The reaction mixture was heated to 130 °C for 3 h and the conversion was monitored by NMR (addition of further amine if necessary). 100 mL of chloroform was added and the organic phase was washed with deionised water (3 x 100 mL) and dried over $MgSO_4$. The solvent was removed and the yellow solid was purified by column chromatography (silica gel, ethyl acetate : MeOH 10 : 1). R_f = 0.3 (EA: MeOH 3:1). A yellow/orange solid was obtain with a yield of 28 % (435 mg).

^{1}H NMR (400 MHz, $CDCl_3$): 8.96 (s, 2H), 4.45 (t, *J* = 5.4 Hz, 4H), 3.83 (t, *J* = 5.5 Hz, 4H), 3.69 – 3.68 (m, 4H), 3.64 – 3.59 (m, 40H), 3.54 – 3.53 (m, 4H), 3.36 (s, 6H). ^{13}C NMR (100 MHz, $CDCl_3$): 161.0, 160.9, 139.2, 128.5, 127.9, 125.5, 124.2, 72.0, 71.0, 70.7 (multiple peaks), 70.2, 68.7, 59.2, 40.1. HRMS (ES-ToF): 1067.2562 [MH^+] (calc. 1067.2599).

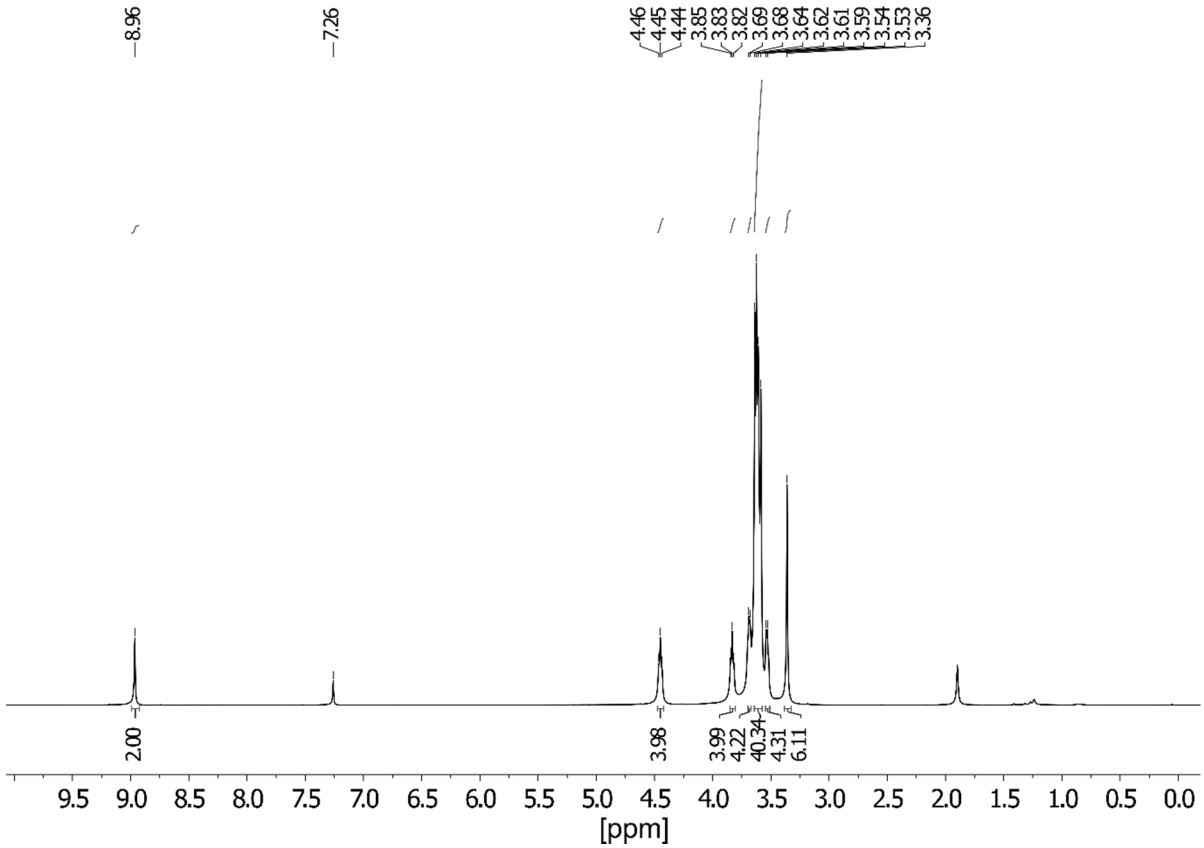

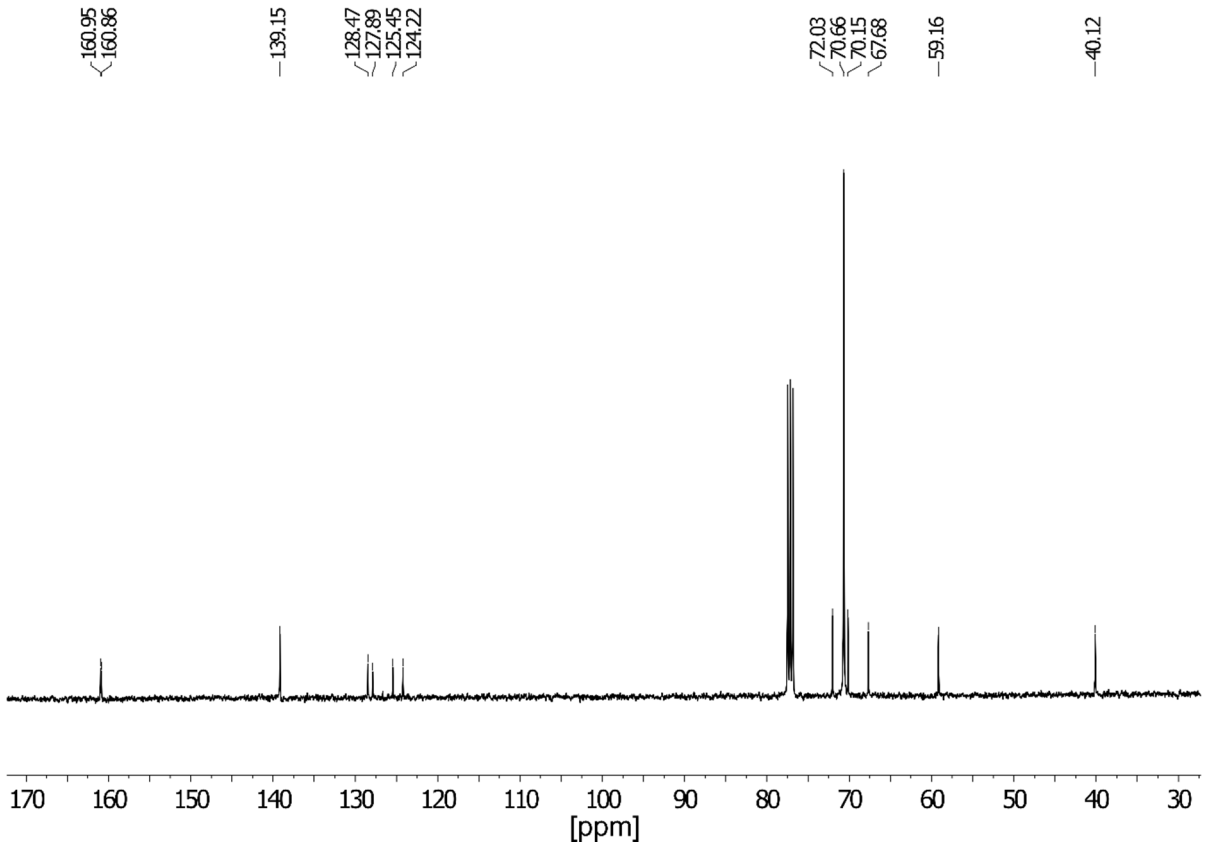

Figure S6: ^{1}H NMR and ^{13}C NMR spectra of **g7-NDI-Br_2** measured in $CDCl_3$.

2.2. Polymer synthesis:

2.2.1. General procedure for polymer synthesis:

In a 2.0 mL microwave vial, the monomer (N,N'-bis(7-glycol)-2,6-dibromonaphthalene-1,4,5,8-bis(dicarboximide) (**g7-NDI-Br$_2$**) and/or N,N'-bis(2-octyldodecyl)-2,6-dibromonaphthalene-1,4,5,8-bis(dicarboximide) and 5,5'-bis(trimethylstannyl)-2,2'-bithiophene were dissolved in 1.5 mL of anhydrous, degassed chlorobenzene. $Pd_2(dba)_3$ (2 mol%) and P(*o*-tol)$_3$ (8 mol%) were added and the vial was sealed and heated to 135 °C for 16 h. After the polymerization was finished, the end-capping procedure was carried out. Then, the reaction mixture was cooled to room temperature and the reaction mixture was precipitated in ethyl acetate followed by addition of hexane. The solid was collected in a glass-fiber thimble and Soxhlet extraction was carried out with hexane, ethyl acetate, MeOH, acetone and chloroform. The polymers dissolved in hot chloroform and the solvent was removed under reduced pressure. Finally, the polymers were precipitated in ethyl acetate and the dark blue solids were dried under high vacuum for 16 h.

2.2.2. General procedure for end-capping:

0.1 mL of a solution made of 0.1 mL 2-(Tributylstannyl)thiophene in 0.5 mL of chlorobenzene and 0.5 mg of $Pd_2(dba)_3$ was added and heated for 1 h to 135 °C, then 0.1 mL of a solution made of 0.1 mL 2-bromothiophene in 0.5 mL of chlorobenzene was added and heated for 1 h to 135 °C.

P-100: The general procedure was applied to prepare polymer **P-100** with (N,N'-bis(7-glycol)-2,6-dibromonaphthalene-1,4,5,8-bis(dicarboximide) (40.25 mg, 37.65 µmol) and 5,5'-bis(trimethylstannyl)-2,2'-bithiophene (18.52 mg, 37.65 µmol). Polymer **P-100** was obtained as a dark blue solid with a yield of 48 % (19.4 mg, 18.1 µmol).

GPC (chlorobenzene, 80 °C): M_n = 7.2 kDa, M_w = 9.0 kDa.

^{1}H NMR ($CDCl_3$, 400 MHz) δ: 8.82 (s, 2 H), 7.36 (broad s, 4 H), 4.45 (broad s, 4 H), 3.84 (broad s, 4 H), 3.71 (broad s, 4 H), 3.62 – 3.62 (m, 40 H), 3.53 (broad s, 4 H), 3.36 (broad s, 6 H) ppm.

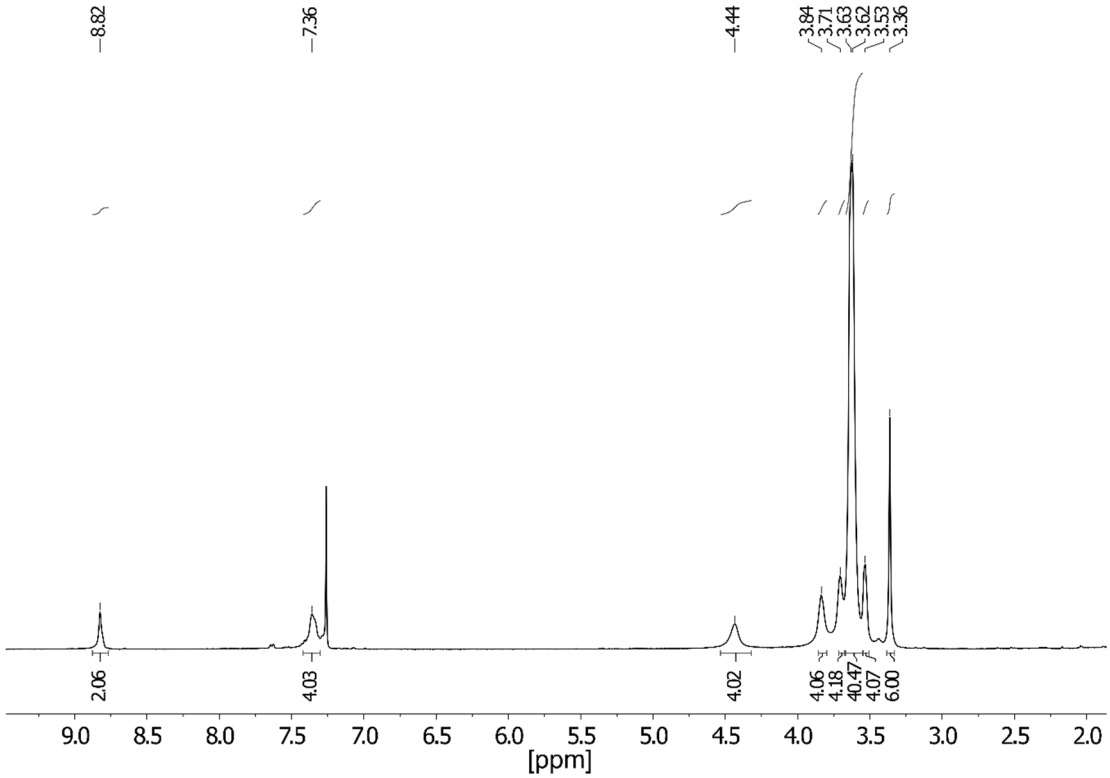

Figure S7: ^{1}H NMR spectrum of **P-100** measured in $CDCl_3$.

P-90: The general procedure was applied to prepare polymer **P-90** with N,N'-bis(7-glycol)-2,6-dibromonaphthalene-1,4,5,8-bis(dicarboximide) (115.36 mg, 107.93 µmol), N,N'-bis(2-octyldodecyl)-2,6-dibromonaphthalene-1,4,5,8-bis(dicarboximide) (11.85 mg, 12.03 µmol), 5,5'-bis(trimethylstannyl)-2,2'-bithiophene (59.16 mg, 120.28 µmol). Polymer P-90 was obtained as a dark blue solid in a yield of 70%. (88.6 mg, 83.2 µmol).

GPC (chlorobenzene, 80 °C): M_n = 7.8 kDa, M_w = 12.4 kDa.

^{1}H NMR ($CDCl_3$, 400 MHz) δ: 8.82 (s, 2H), 7.35 (m, 4.0 H), 4.44 (broad s, 3.60 H), 4.12 (broad s, 0.4 H) 3.85– 3.82 (m, 3.6 H), 3.72– 3.70 (m, 3.6 H), 3.64 – 3.62 (m, 36 H), 3.54 – 3.52 (m, 3.6 H), 3.36 (m, 5.4 H) ppm, 2.00 (broad s, 0.2 H), 1.25-1.23 (m, 6.4 H), 0.85 (broad s, 1.2 H).

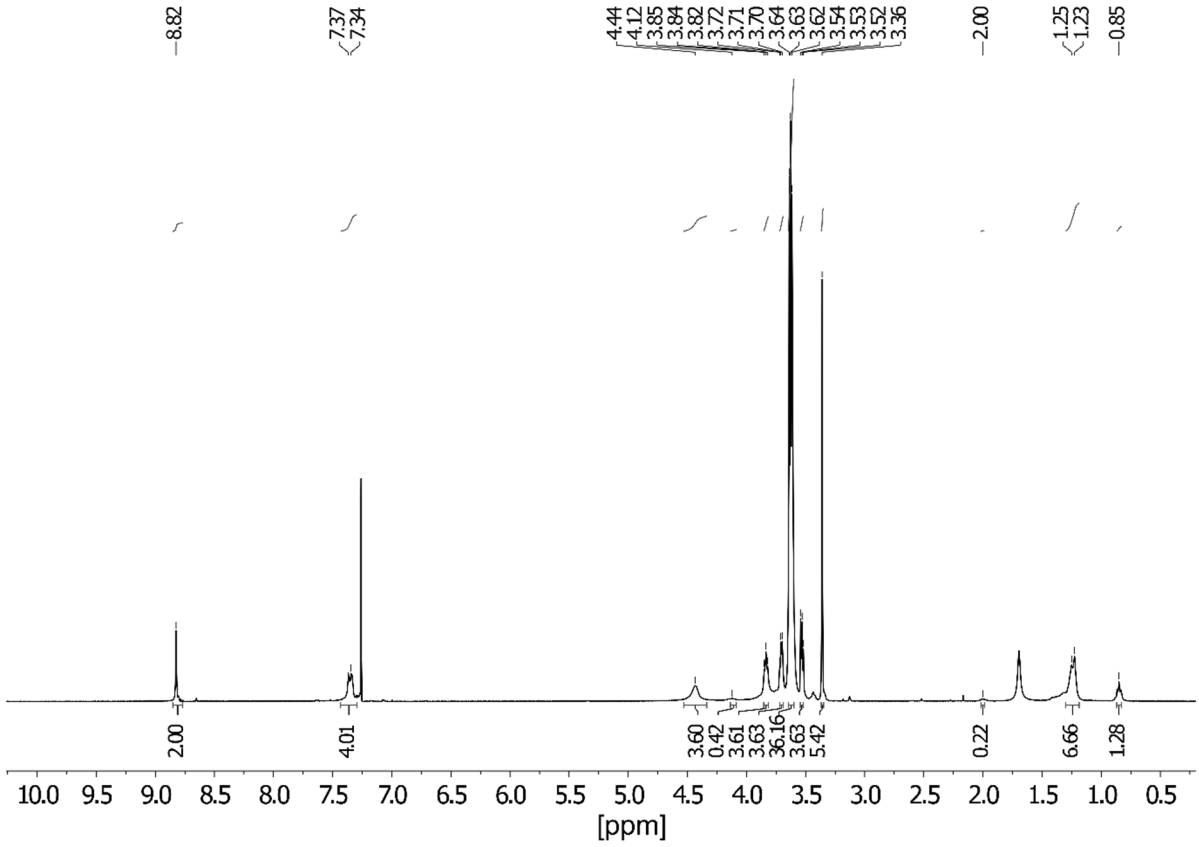

Figure S8: ^{1}H NMR spectrum of **P-90** was measured in $CDCl_3$.

P-75: The general procedure was applied to prepare polymer **P-75** with N,N'-bis(7-glycol)-2,6-dibromonaphthalene-1,4,5,8-bis(dicarboximide) (74.93 mg, 70.11 µmol), N,N'-bis(2-octyldodecyl)-2,6-dibromonaphthalene-1,4,5,8-bis(dicarboximide) (23.05 mg, 23.40 µmol), 5,5'-bis(trimethylstannyl)-2,2'-bithiophene (46.00 mg, 3.52 µmol). Polymer **P-75** was obtained as a dark blue solid in a yield of 76%. (74.6 mg, 70.8 µmol).

GPC (chlorobenzene, 80 °C): M_n = 10.7 kDa, M_w = 22.8 kDa.

^{1}H NMR ($CDCl_3$, 400 MHz) δ: 8.82 (s, 2H), 7.35 (s, 16 H), 4.43 (broad s, 3 H), 4.12 (broad s, 1 H) 3.85 (3, 3 H), 3.72 (m, 3 H), 3.64 – 3.62 (m, 30 H), 3.54-3.52 (m, 3.0 H), 3.36 (m, 4.5 H) ppm, 2.00 (broad s, 0.5 H), 1.44-1.16 (m, 16 H), 0.90-0.80 (m, 3 H).

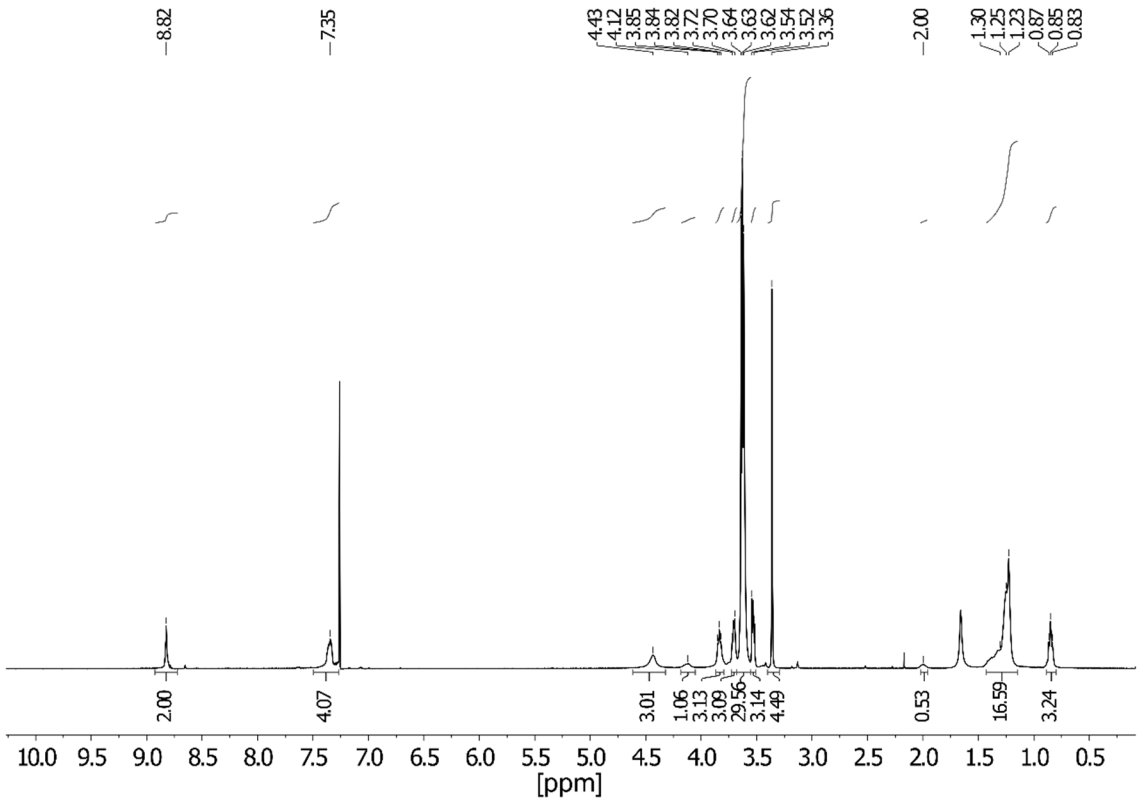

Figure S9: ^{1}H NMR spectrum of **P-75** measured in $CDCl_3$.

P-50: The general procedure was applied to prepare polymer **P-50** with N,N'-bis(2-octyldodecyl)-2,6-dibromonaphthalene-1,4,5,8-bis(dicarboximide) (27.22 mg, 27.63 µmol), N,N'-bis(7-glycol)-2,6-dibromonaphthalene-1,4,5,8-bis(dicarboximide) (29.54 mg, 27.63 µmol) and 5,5'-bis(trimethylstannyl)-2,2'-bithiophene (27.19 mg, 55.27 µmol). Polymer **P-50** was obtained as a dark blue solid with a yield of 54 % (30 mg, 29.1 mmol).

GPC (chlorobenzene, 80 °C): M_n = 19 kDa, M_w = 31 kDa.

^{1}H NMR ($CDCl_3$, 400 MHz) δ: 8.81 (s, 2 H), 7.34 (s, 4 H), 4.43 (broad s, 2 H), 4.12 (broad s, 2 H), 3.83 (broad s, 2 H), 3.70 (broad s, 2 H), 3.63 – 3.61 (m, 20 H), 3.53 (broad s, 2 H), 3.36 (broad s, 3 H), 1.99 (broad s, 1 H), 1.48 – 1.15 (m, 32 H), 0.91 – 0.77 (m, 6 H).

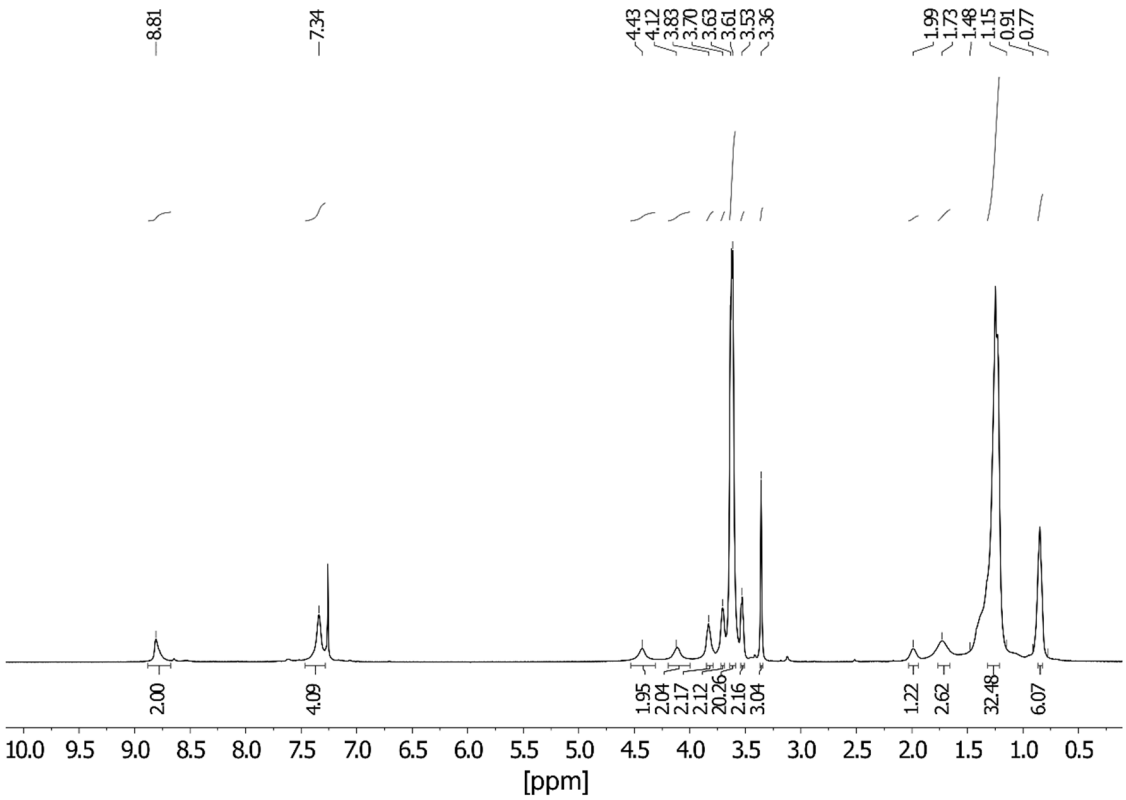

Figure S10: ^{1}H NMR spectrum of p(NDI-T2-50%) in $CDCl_3$.

P-25: The general procedure was applied to prepare polymer **P-25** with N,N'-bis(2-octyldodecyl)-2,6-dibromonaphthalene-1,4,5,8-bis(dicarboximide) (43.77 mg, 43.44 µmol), N,N'-bis(7-glycol)-2,6-dibromonaphthalene-1,4,5,8-bis(dicarboximide) (15.83 mg, 14.81 µmol) and 5,5'-bis(trimethylstannyl)-2,2'-bithiophene (29.14 mg, 59.24 µmol). Polymer **P-25** was obtained as a dark blue solid with a yield of 50 % (30.0 mg, 29.7 mmol).

GPC (chlorobenzene, 80 °C): M_n = 15.3 kDa, M_w = 27.1 kDa.

^{1}H NMR ($CDCl_3$, 400 MHz) δ: 8.82 (s, 2 H), 7.34 (s, 4 H), 4.44 (broad s, 1 H), 4.12 (broad s, 3 H), 3.83 (broad s, 1 H), 3.71 (broad s, 1 H), 3.64 – 3.61 (m, 10 H), 354– 3.52 (m, 1 H), 3.36 (broad s, 1.5 H), 1.99 (broad s, 1.5 H), 1.48 – 1.15 (m, 46 H), 0.91 – 0.77 (m, 9 H) ppm.

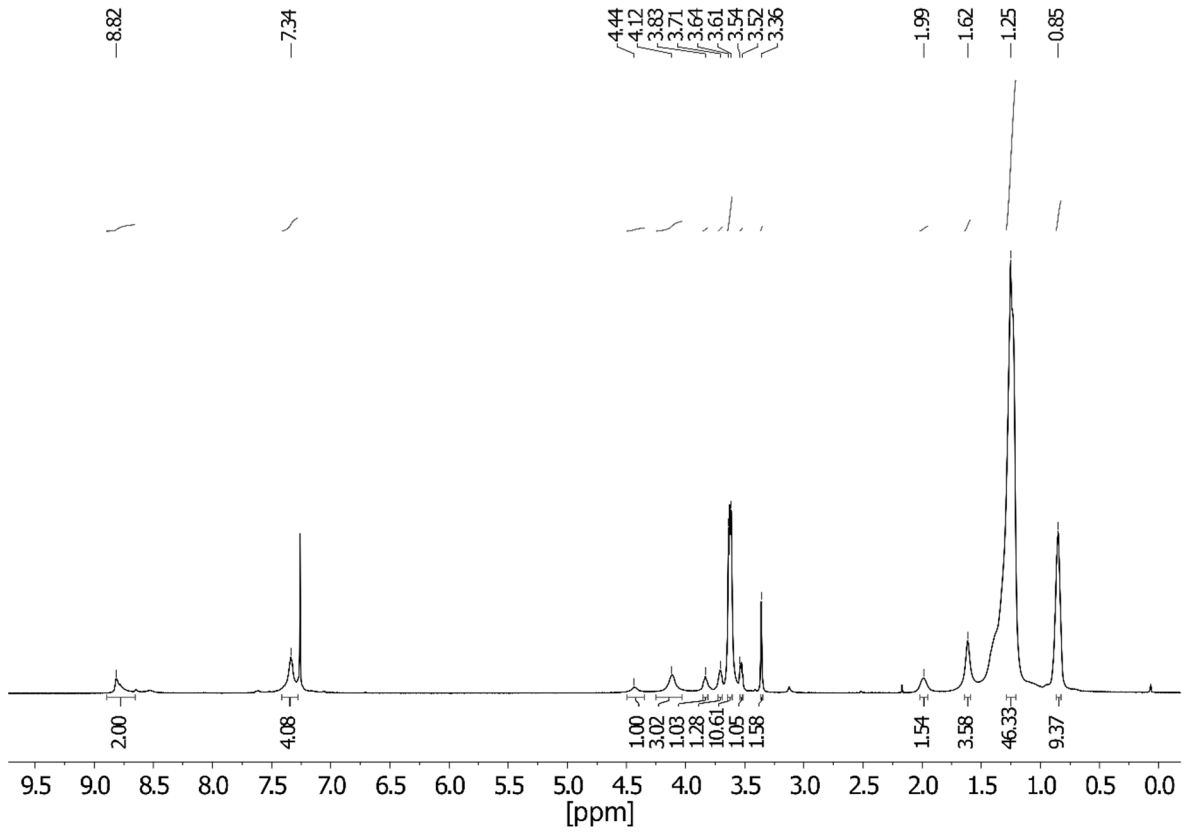

Figure S11: ^{1}H NMR spectrum of **P-25** was measured in $CDCl_3$.

P-10: The general procedure was applied to prepare polymer **P-10** with N,N'-bis(2-octyldodecyl)-2,6-dibromonaphthalene-1,4,5,8-bis(dicarboximide) (56.66 mg, 57.52 µmol), N,N'-bis(7-glycol)-2,6-dibromonaphthalene-1,4,5,8-bis(dicarboximide) (6.83 mg, 6.39 µmol) and 5,5'-bis(trimethylstannyl)-2,2'-bithiophene (31.43 mg, 63.90 µmol). Polymer **P-10** was obtained as a dark blue solid with a yield of 55 % (35 mg, 35.1 mmol).

GPC (chlorobenzene, 80 °C): M_n = 18.4 kDa, M_w = 32.8 kDa.

^{1}H NMR ($CDCl_3$, 400 MHz) δ: 8.82 (s, 2 H), 7.34 (s, 4 H), 4.44 (broad s, 0.4 H), 4.11 (broad s, 3.6 H), 3.84 (broad s, 0.4 H), 3.71 (broad s, 0.4 H), 3.64 – 3.62 (m, 4 H), 354– 3.52 (m, 0.4 H), 3.36 (broad s, 0.6 H), 1.99 (broad s, 1.8 H), 1.48 – 1.15 (m, 55.8 H), 0.91 – 0.77 (m, 10.8 H) ppm.

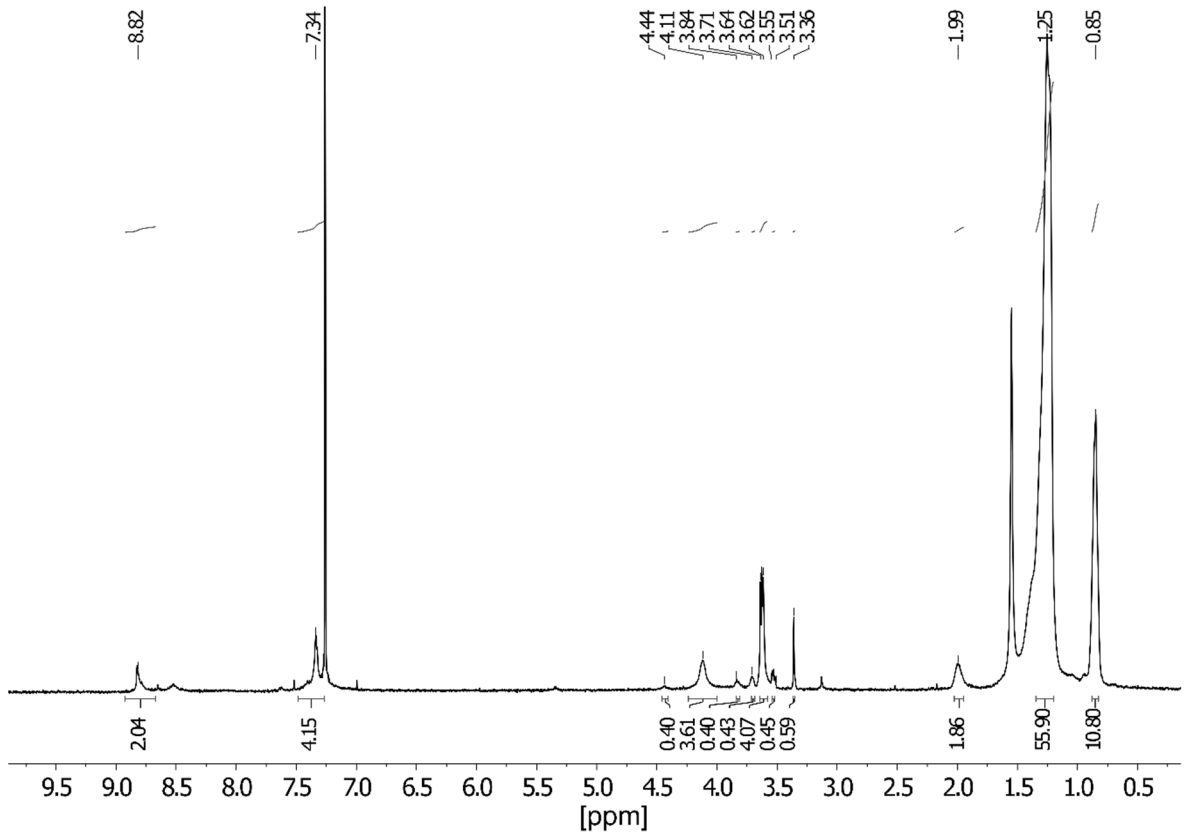

Figure S12: ^{1}H NMR spectrum of **P-10** measured in $CDCl_3$.

P-0: The general procedure was applied to prepare polymer **P-0** with N,N'-bis(2-octyldodecyl)-2,6-dibromonaphthalene-1,4,5,8-bis(dicarboximide) (58.60 mg, 59.49 µmol) and 5,5'-bis(trimethylstannyl)-2,2'-bithiophene (29.26 mg, 59.49 µmol). **P-0** was obtained as a dark blue solid with a yield of 77 % (45.0 mg, 46.0 mmol).

GPC (chlorobenzene, 80 °C): M_n = 18.0 kDa, M_w = 33.0 kDa.

^{1}H NMR ($CDCl_3$, 400 MHz) δ: 8.82 (s, 2 H), 7.34 (s, 4 H), 4.12 (broad s, 4 H), 1.99 (broad s, 2 H), 1.25 (m, 64 H), 0.85 (broad s, 12 H) ppm.

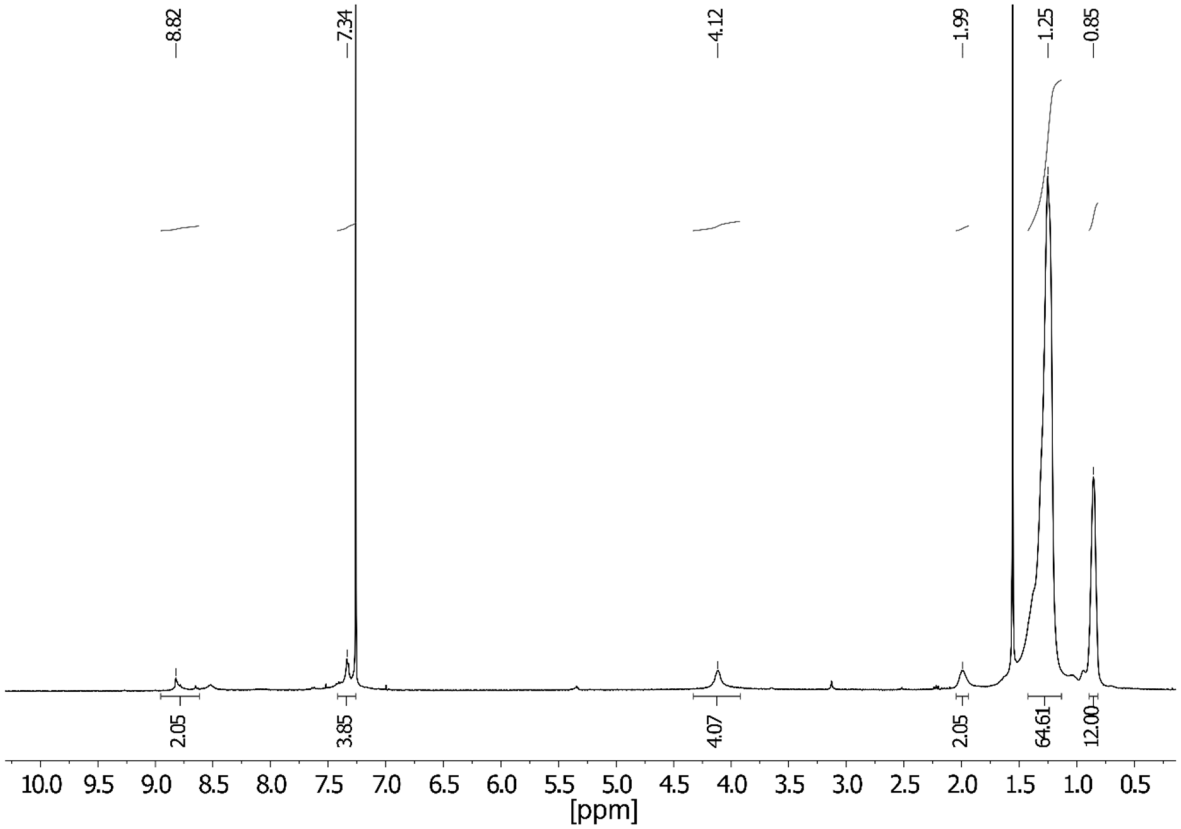

Figure S13: ^{1}H NMR spectrum of **P-0** measured in $CDCl_3$.

2.3. Reaction screening of the NDI formation in different solvents

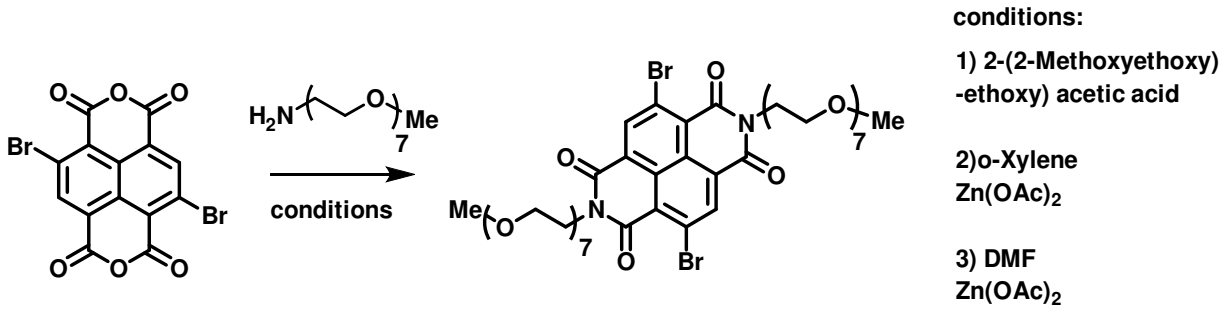

The reaction control by ^{1}H NMR spectroscopy of the different reaction conditions is shown in Figure S14. It can be observed that the diimide formation is highly sensitive to the choice of the solvent. The nucleophilic aromatic substitution (S_NAr) progresses at a faster rate when polar solvents such as DMF or 2-(2-methoxyethoxy)-ethoxy) acetic acid are used compared to *o*-xylene which is a non-polar solvent.

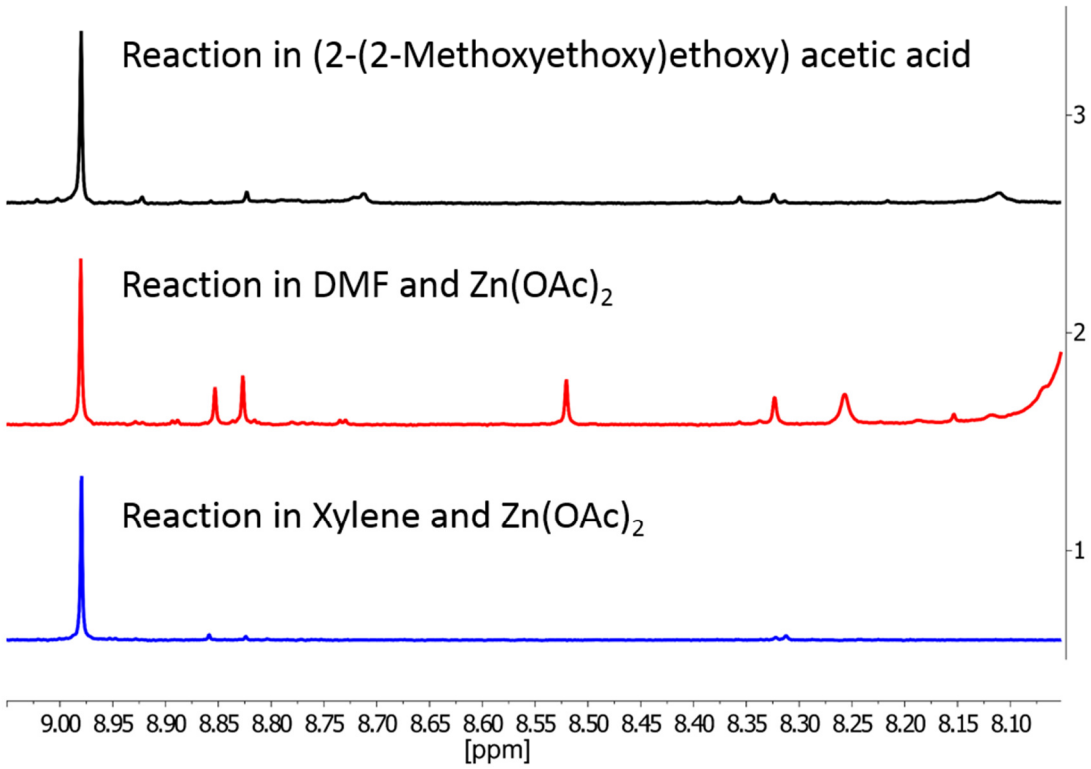

Figure S14: Reaction control by ^{1}H NMR spectroscopy after heating the reaction to 125 °C for 4 h.

3. NMR measurements of the copolymers

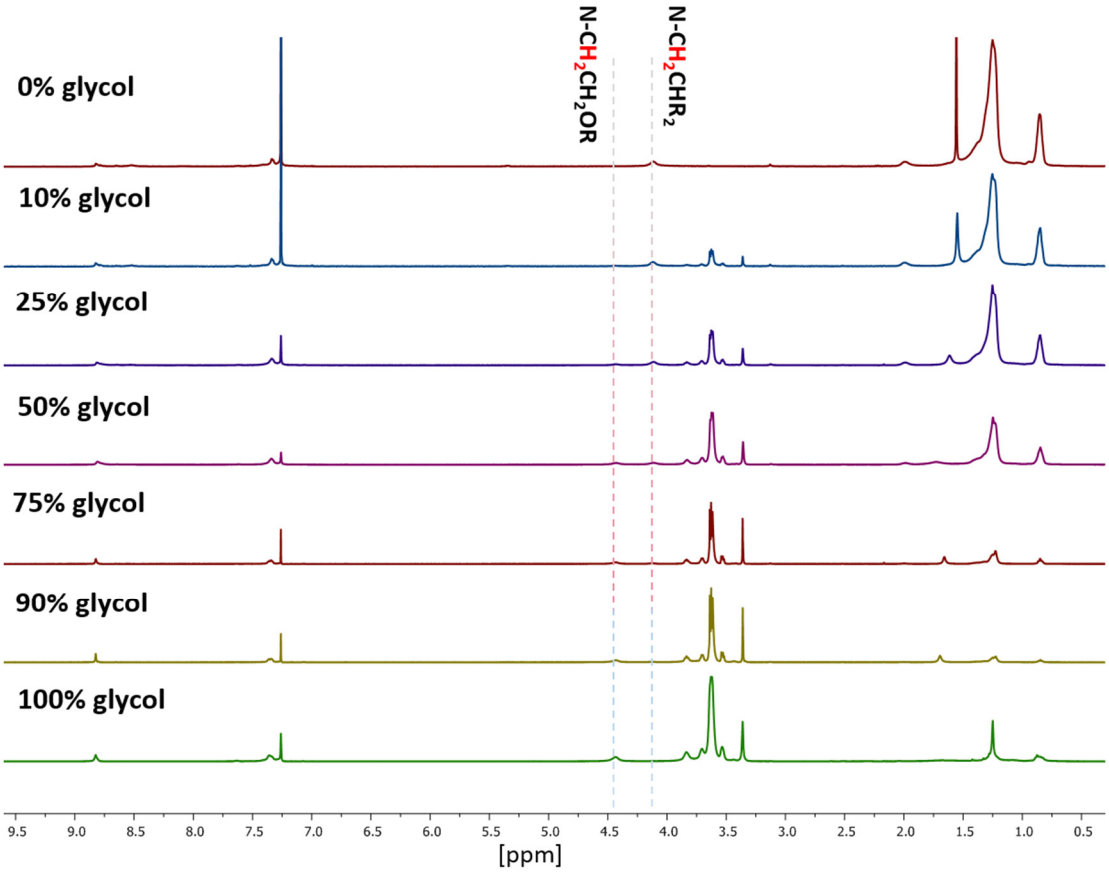

Figure S15: ^{1}H-NMR spectra of the copolymers measured in $CDCl_3$.

4. UV-Vis absorbance spectroscopy

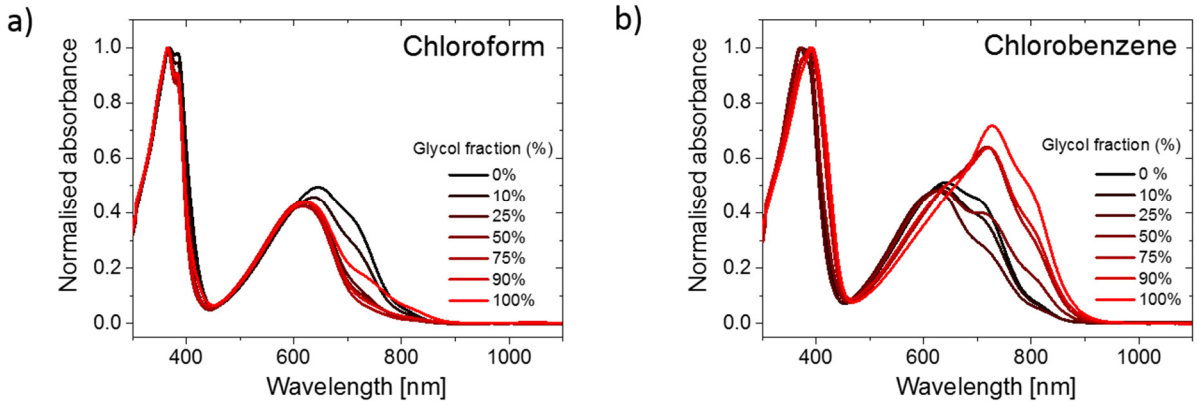

Figure S16: UV-Vis absorbance spectra of the copolymers in a) chloroform and b) chlorobenzene.

5. GPC measurements

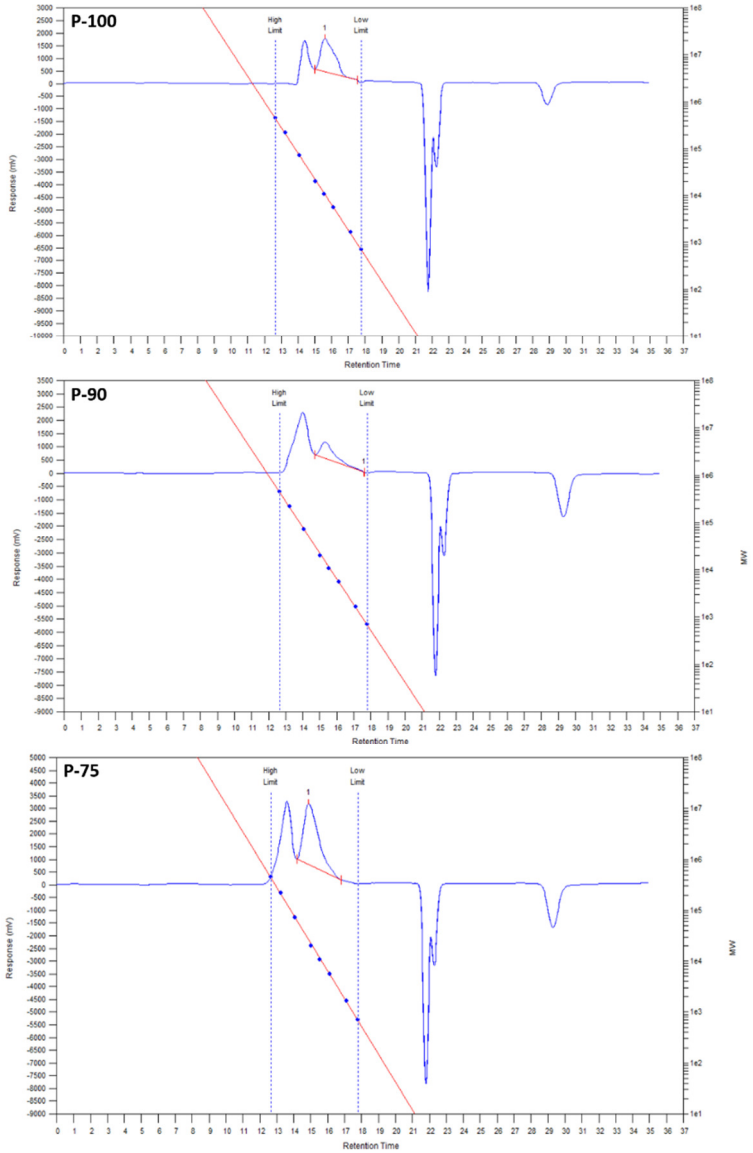

Figure S17: GPC measurements of the polymer **P-100**, **P-90** and **P-75** in chlorobenzene where a bimoduale eluation can be observed where the second peak was used to avoid overestimation of the molecular weight.

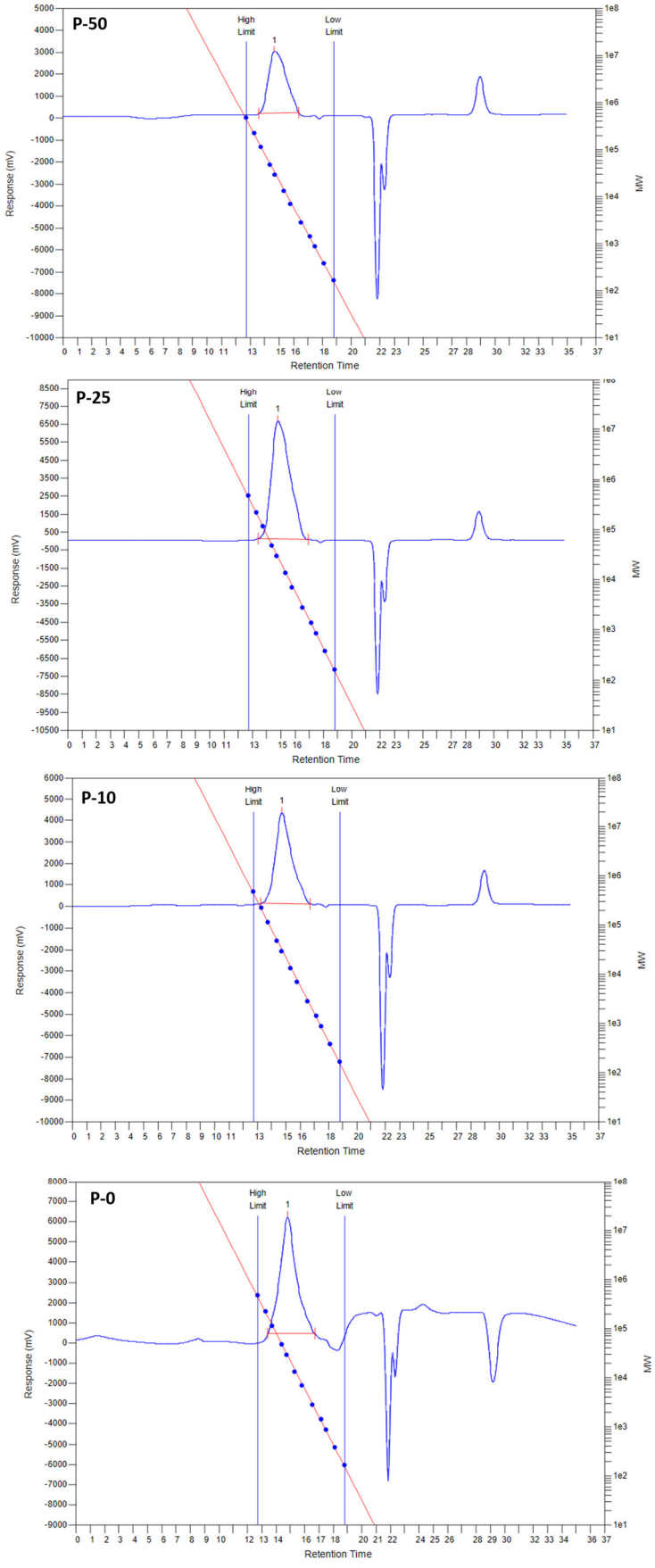

Figure S18: GPC measurements of the polymer **P-50** to **P-0** in chlorobenzene (no observation of a bimoduale eluation).

6. Mass spectrometry (MALDI-ToF)

MALDI-ToF measurements were carried out in negative linear mode with DTCB as the matrix.

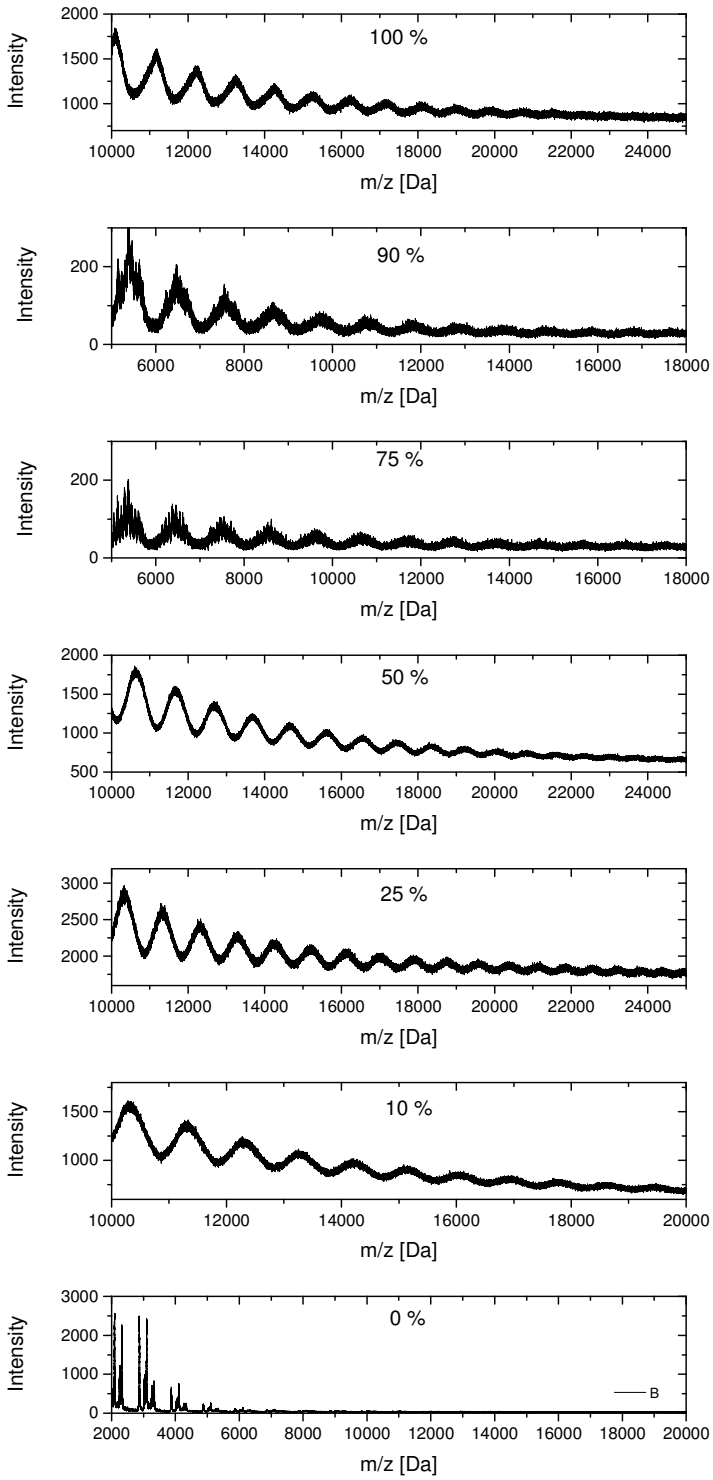

Figure S19: MALDI ToF spectra of the copolymers.

7. PDS measurements

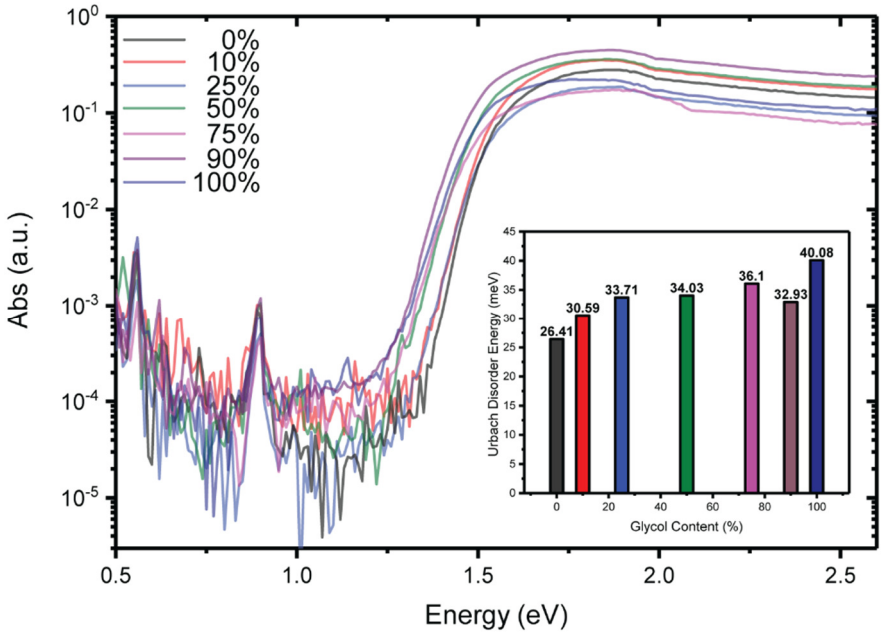

Figure S20: PDS measurements of the polymer series with the Urbach disorder energies (inset).

8. Photoluminescence measurements and corrections:

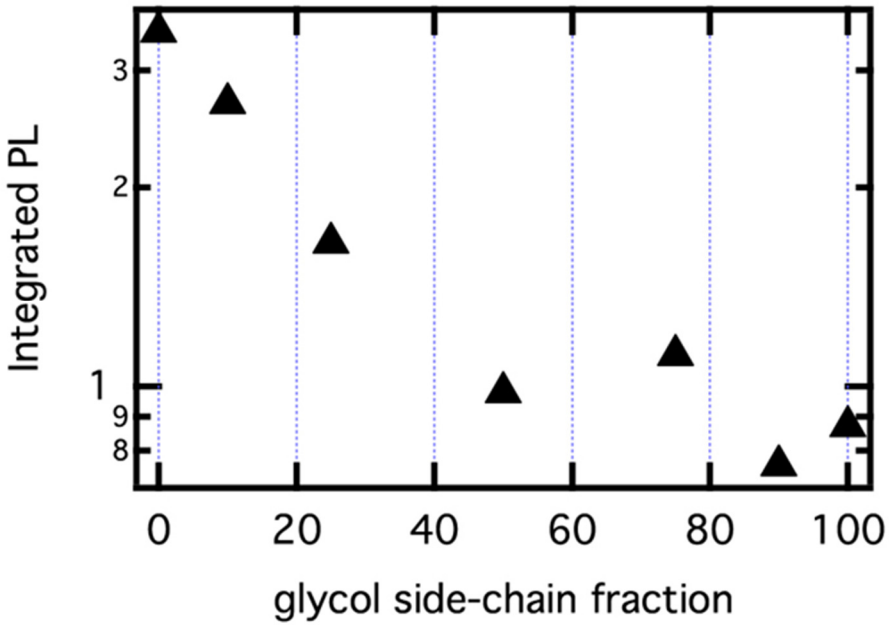

Figure S21: Integrated thin-film photoluminescence intensity as a function of glycol side-chain fraction (%).

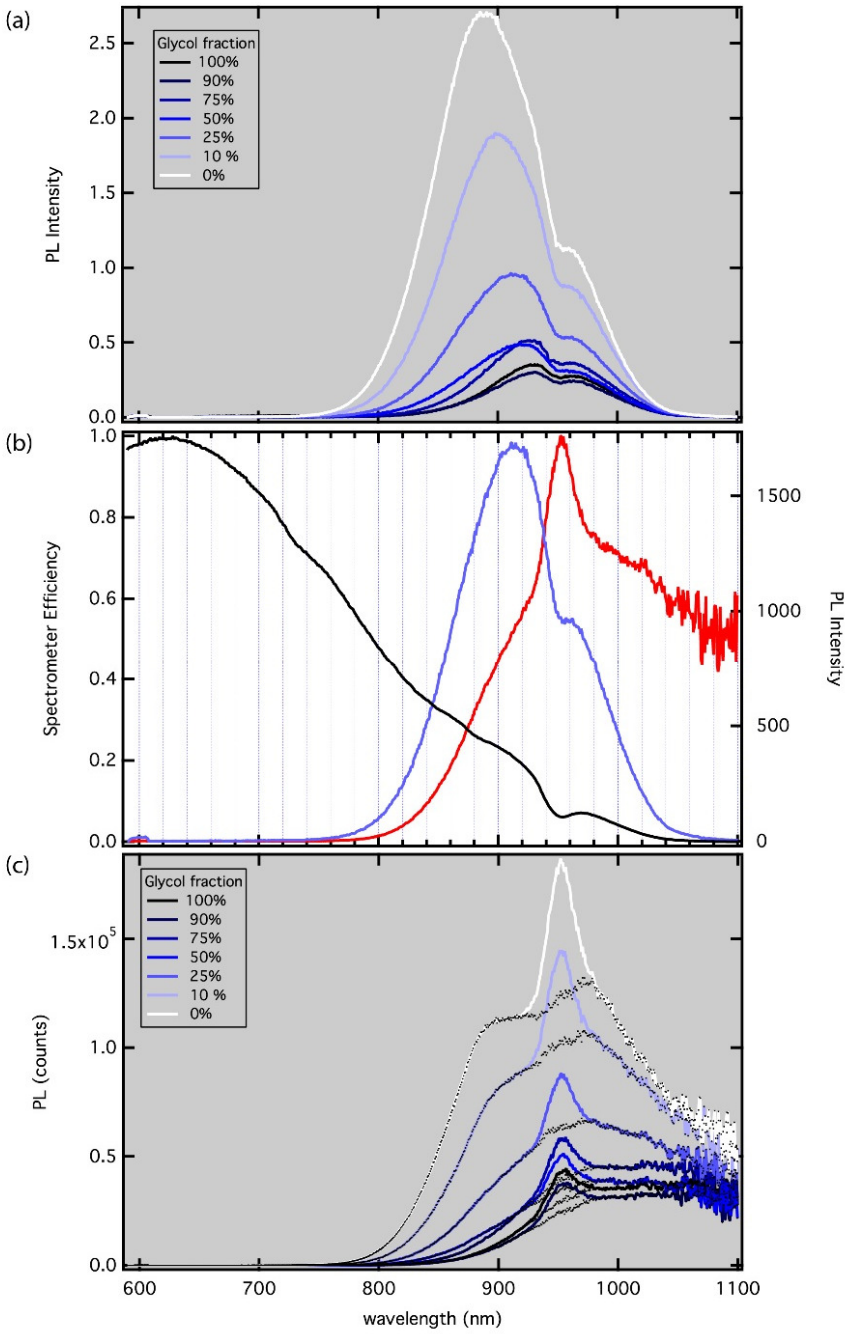

Figure S22: (a) Raw photoluminescence spectra of p(NDI-T2) thin-films for the range of glycol side-chain fractions shown in the legend. (b) The spectrometer efficiency correction curve (black trace, left axis), and one raw PL spectrum (blue trace) with the corresponding corrected spectrum (red trace). (c) Corrected PL spectra for all samples (colored traces) and the same spectra after subtraction of a suspected grating artifact (black dotted traces) that was not properly removed using the measured correction curve in (b). The subtraction was performed by fitting the corrected spectra with multiple Gaussian functions (3-4), and subtracting the one accounting for the grating artifact. The black dotted traces are what is shown in the main text. Although this methodology for correcting the measured PL spectra is far from perfect, we believe that it provides a better approximation of the true PL spectra than the raw data. Importantly, the trends that we observe, red shift and quenching, are unaffected by corrections we apply.

9. Thermogravimetric analysis

Polymers were heated under inert conditions (nitrogen flow) under the following conditions: [1] 30.0 to 105.0 °C, 34.99 K/min, N_2 50.0 ml/min, [2] 105.0 °C, 10.00 min N_2 50.0 ml/min [3] 105.0 to 800.0 °C, 10.00 K/min N_2 50.0 ml/min

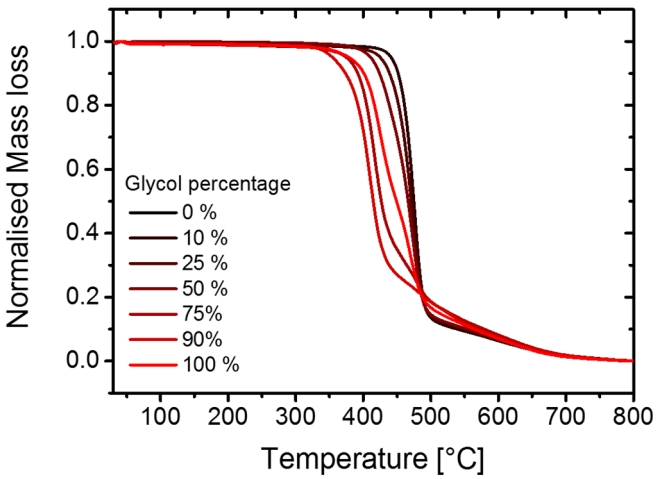

Figure S23: TGA of the copolymers.

10.Differential scanning calorimeter (DSC)

Conditions: -30 °C to 330 °C, heating/cooling rate 10 °C/min under nitrogen atmosphere.

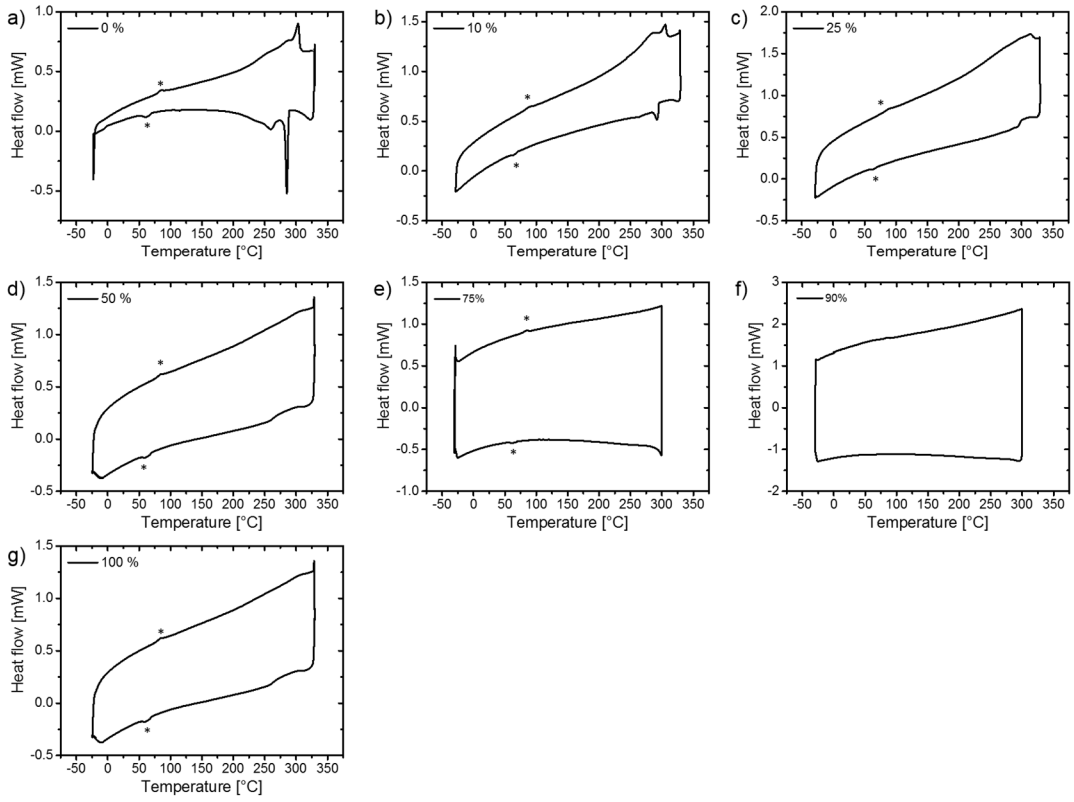

Figure S24: DSC measurements of the polymer series (first cycle is shown), artifacts (labeled as *) at 80-85 °C (heating) and 60-65 °C (cooling) are present in all measurements and are not related to events during the heating/cooling cycles.

11.CV measurements in aqueous solutions

Thin films of the copolymers on FTO coated glass substrates were prepared by spin coating from chloroform (5mg/mL). The films were then exposed to a degassed 0.1 M NaCl solution and five charging and discharging cycles were carried out at a scan rate of 100 mV/s vs Ag/AgCl. The electrolyte was degassed with argon.

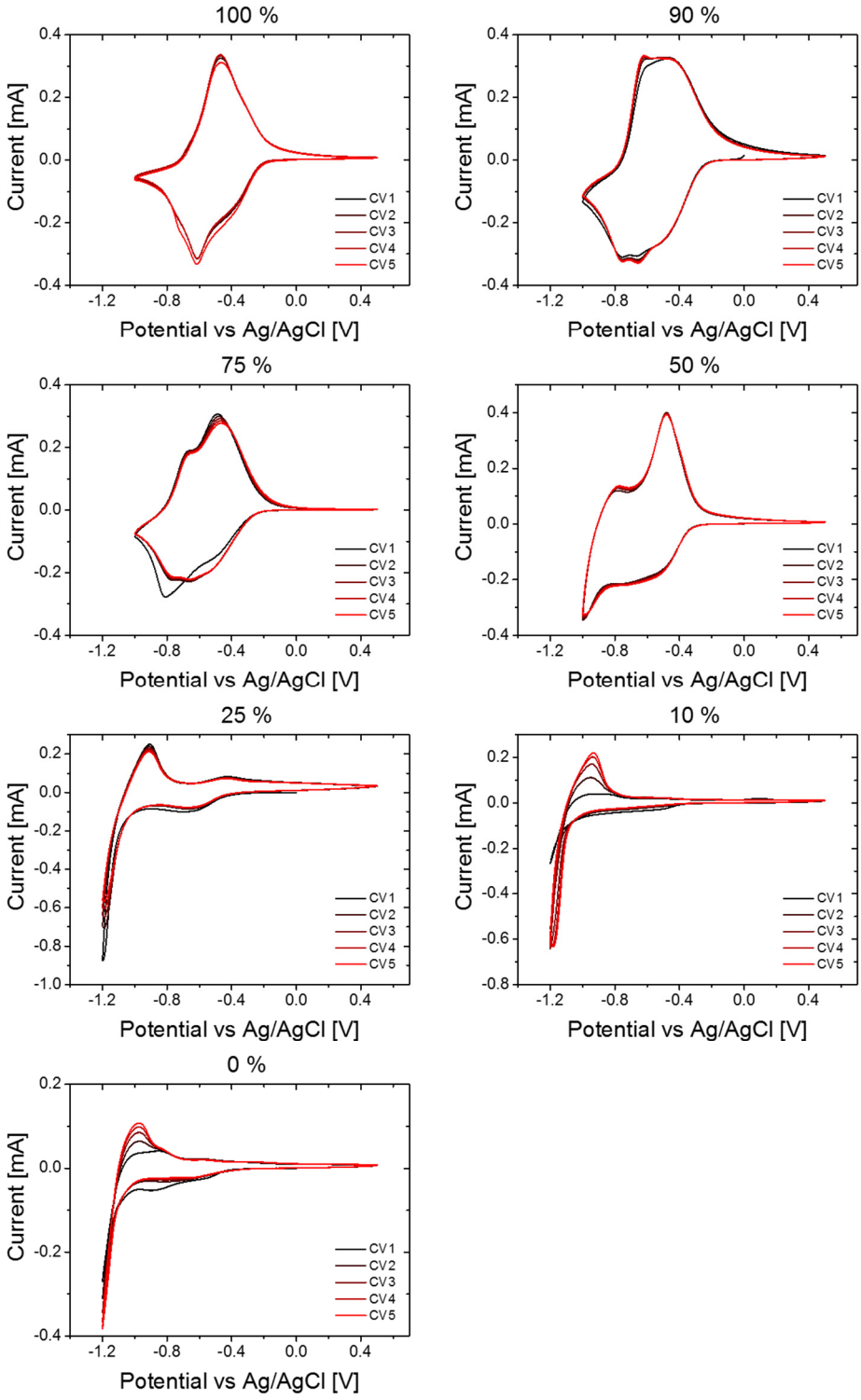

Figure S25: CV measurements of the polymers on FTO (5 cycles) in 0.1 M NaCl aqueous solutions.

12.Electrical impedance measurements (EIS)

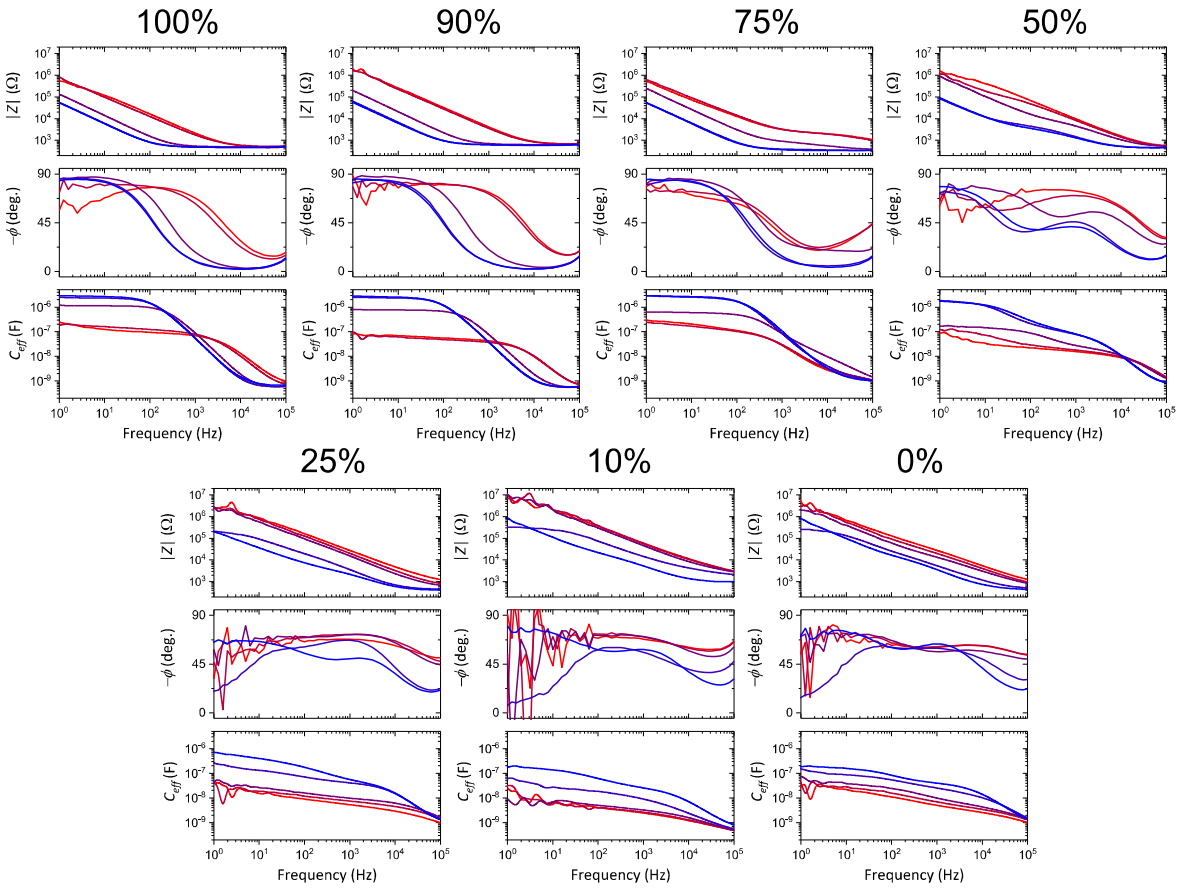

Figure S26: Electrochemical impedance spectroscopy. Bode plots (|Z| vs frequency, and phase vs. frequency) as well as the effective capacitance for **P-0**, **P-10**, **P-25**, **P-50**, **P-75**, **P-90** and **P-100**. The color codes denote the offset working electrode bias from red to blue (0.2, 0, -0.2, -0.4, -0.6V). All devices were measured on a coated gold electrode with area and thicknesses as reported in Table 2 (main text.)

13.OECT performance

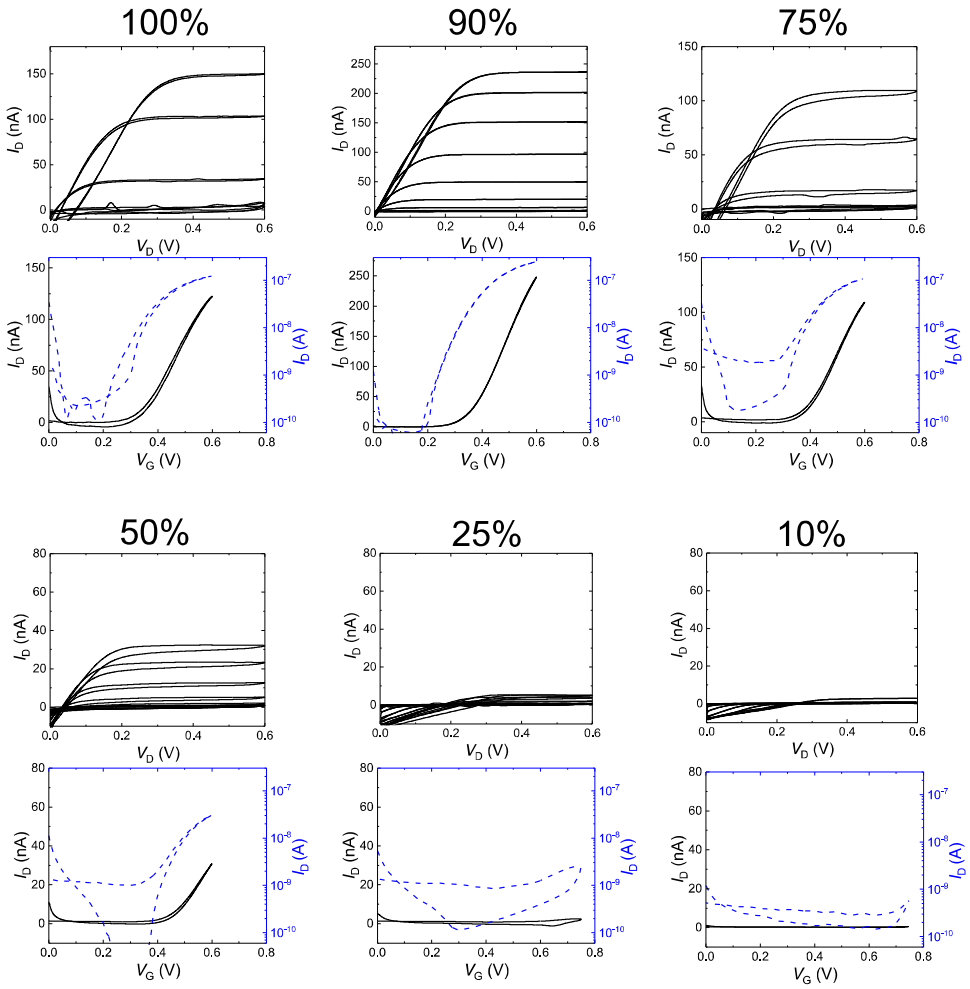

Figure S27: Organic electrochemical transistor measurements for **P-10**, **P-25**, **P-50**, **P-75**, **P-90** and **P-100**. For each polymer, the output (I_D-V_D) and transfer (I_D-V_G; linear, black solid line, log scale, blue dotted line) plots are shown. All OECTs measured were nominally 100x10 µm (*W*x*L*), with thicknesses of 28 nm (**P-100**), 52 nm (**P-90**), 39 nm (**P-75**), 31 nm (**P-50**), 32 nm (**P-25**), and 41 nm (**P-10**). **P-0** did not show OECT operation, or any indications of turn on over the bias range probed. The non-idealities typically observed for NDI copolymers with polar side chains (**P-50** to **P-100** as well as **p(gNDI-gT2)**[5]) are often associated with voltages that lead to irreversible degradation, and are the topic of ongoing investigation. The typical operation voltages (peak g_m), are at stable potentials.

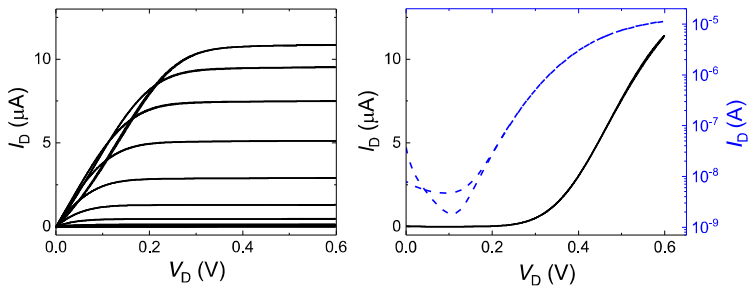

Figure S28: Thickness scaling for OECT performance. **P-90** OECT with the same areal dimensions (100x10 µm), as spin cast devices above, with a thickness of 1015nm. This OECT yields a peak transconductance, g_m, of 47 µS.

14. OFET measurements

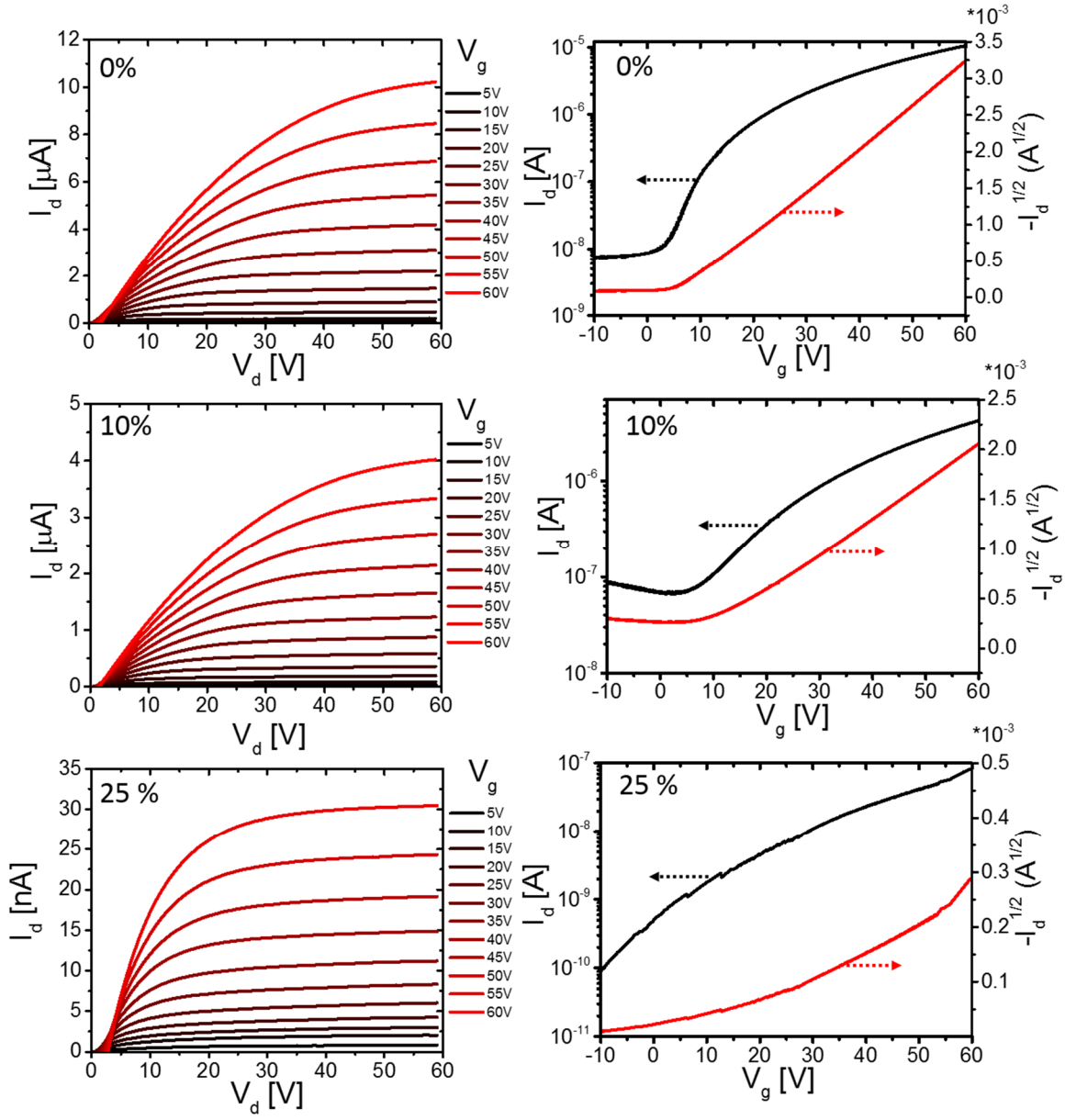

Figure S29: Output and transfer curves of **P-0**, **P-10** and **P-25** measured in OFETs.

15.Microwave conductivity photoconductance transients measurements

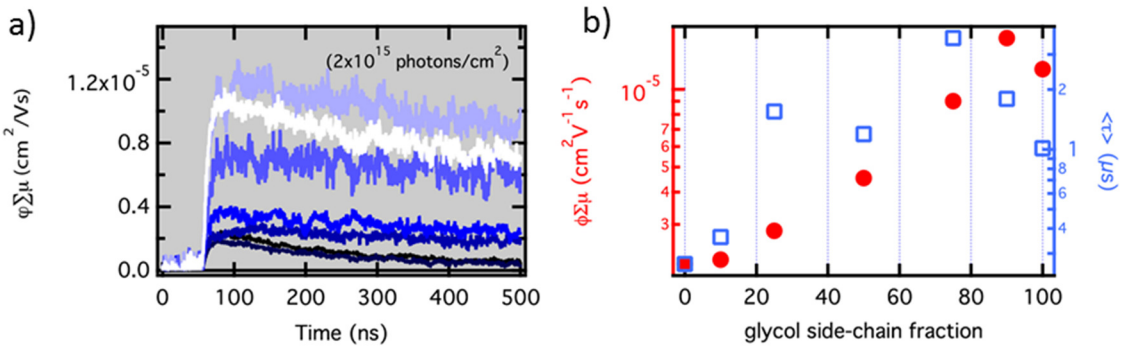

Figure S30: (a) Microwave photoconductance transients measured with 700 nm excitation at $2x10^{15}$ photons/cm^2. The left axis is an expression of the fluence-normalized photoconductance, the product of carrier yield and the sum of microwave-frequency mobility contributions. (b) The initial magnitude (red circles, left axis) and single-exponential lifetime (blue squares, right axis) as a function of glycol side-chain fraction (%). These values were extracted from single-exponential fits to each transient, and averaged across the measured intensity range ($2x10^{14}$ – $2x10^{15}$ cm^{-2}) as there was little variation in either property as a function of intensity.

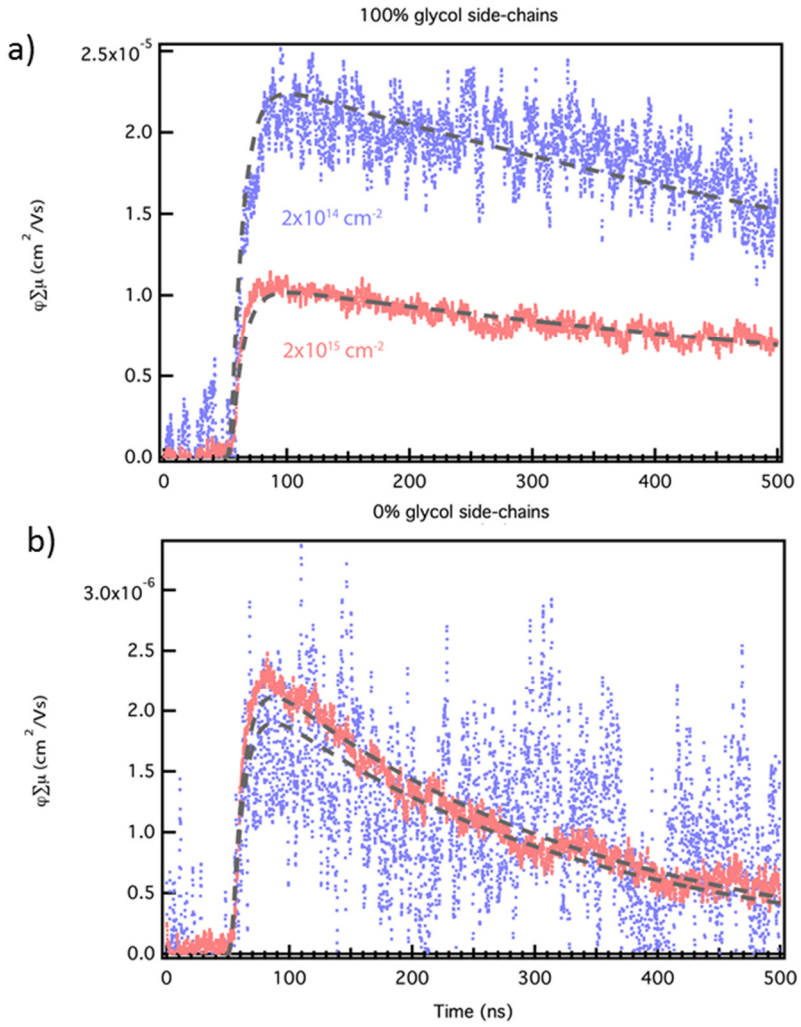

Figure S31: Example microwave photoconductance transients for thin films of **P-100:** (a) and P-0 (b) glycol side-chain fraction. The red traces show the results for excitation with $2x10^{15}$ cm^{-2} and the blue for $2x10^{14}$ cm^{-2}. The gray dashed traces show the single-exponential fits used to calculate the data points in Figure S28.

16. GIWAXS

The 2D GIXS, line cuts and tables of extracted values are shown below; notable variation for samples **P-75**, and **P-90** are found due to variable background scattering and beam stop effects, separate from the other samples which were tested in a different run.

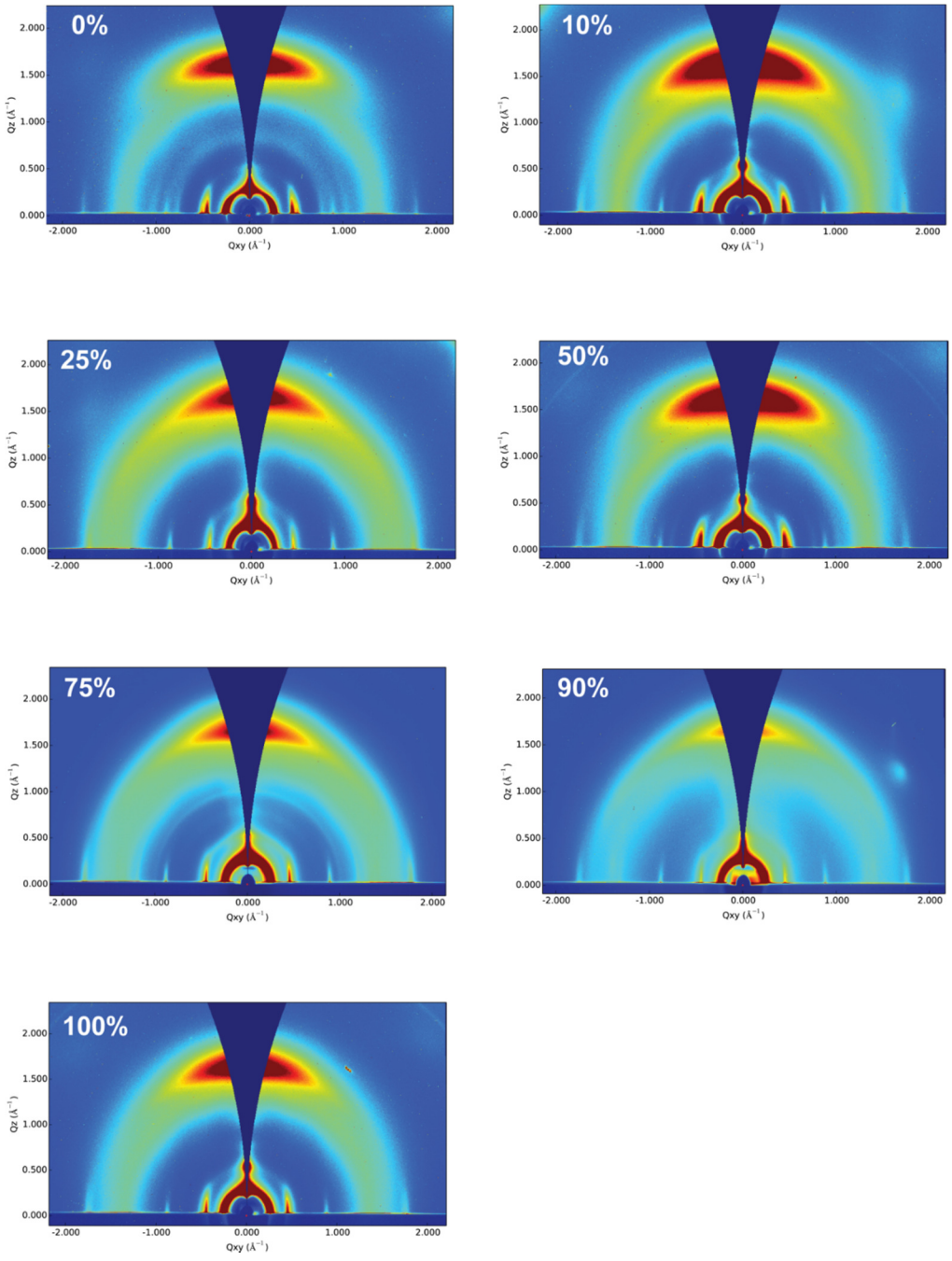

Figure S32: 2D GIWAXS patterns for **P-0** – **P-100**. All films are as cast, not electrochemically switched, and testing in He environment to reduce scattering

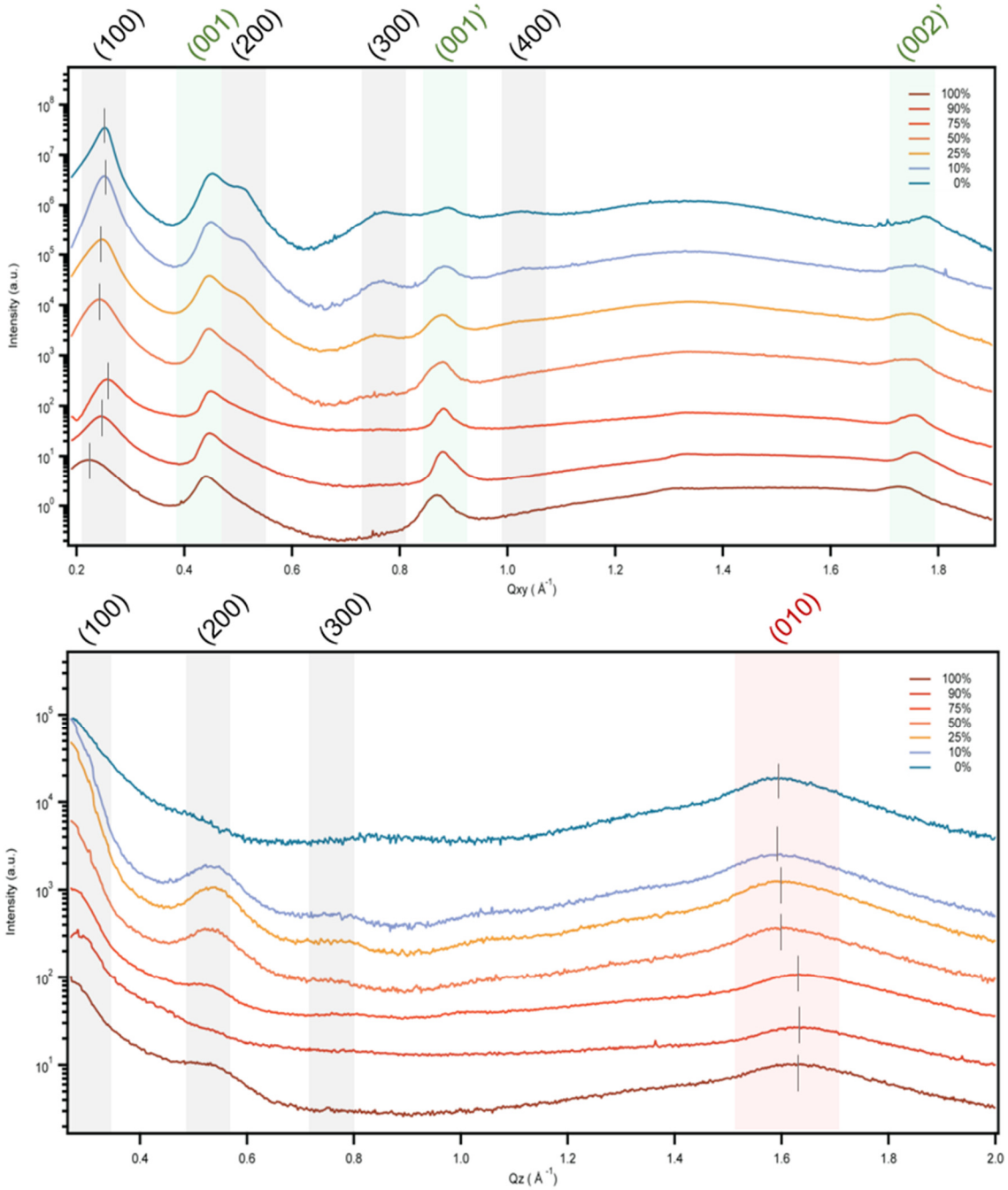

Figure S33: Horizontal (Q_{xy}), top, and vertical (Q_z), bottom, linecuts for **P-0** – **P-100**, with indexing denoted. Black indexing denotes (h00), lamellar stacking peaks; green (00l) denotes backbone-related scattering, and red (0k0) denotes pi-stacking scattering.

Table S1 of values extracted from 2D line cuts in Figure S33.

% glycol	(100) in plane		(010) pi-stack, out of plane					(001) in plane		(001)' in plane		$A_{(001)'}/A_{(001)}$
	q (Å^{-1})	d (Å)	q (Å^{-1})	d (Å)	Δ_q (Å^{-1})	L_c (Å)	g (%)	q (Å^{-1})	d (Å)	q (Å^{-1})	d (Å)	
0	0.25	25.2	1.60	3.92	0.242	26.0	15.5	0.45	13.9	0.89	7.06	0.07
10	0.25	25.1	1.58	3.97	0.173	36.3	13.2	0.45	13.9	0.89	7.07	0.08
25	0.25	25.6	1.61	3.91	0.256	24.5	15.9	0.45	14.1	0.88	7.16	0.24
50	0.24	26.0	1.62	3.88	0.256	24.5	15.7	0.45	14.1	0.88	7.17	0.36
75	0.26	24.3	1.62	3.88	0.294	21.3	17.0	0.45	14.0	0.88	7.14	0.56
90	0.25	25.1	1.66	3.79	0.205	30.6	14.1	0.46	13.7	0.89	7.04	0.35
100	0.23	27.8	1.63	3.87	0.301	20.9	17.2	0.45	14.1	0.87	7.20	0.33

q is the peak position in reciprocal space, d is the corresponding spacing where $d=2\pi/q$. Delta_q is the peak width in reciprocal space, L_c is the coherence length ($L_c=2\pi/\Delta_q$), and g is the single peak estimate of paracrystallinity as in ref(Rivnay, Noriga, PRB) where $g=(1/2\pi)$ sqrt(Δ_q d). $A_{(001)'}/A_{(001)}$ is the peak area ratio of the (001)' (Form I) to (001) (Form II) polymorphs.

17. QCM-D measurements

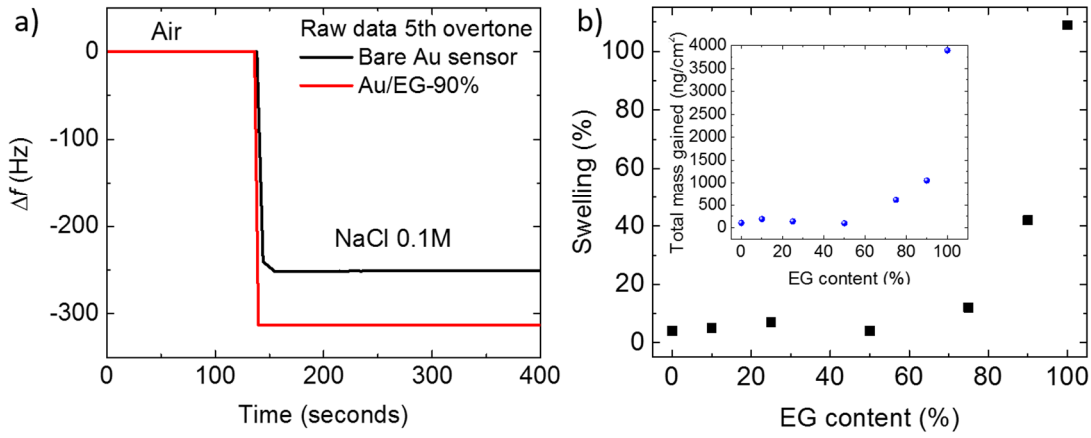

Figure S34: a) Raw QCM-D data for the bare sensor and for the same sensor coated with EG90% polymer before and after exposure to NaCl (0.1M, aqueous). The same data obtained for all the polymers under study and used to accurately determine the swelling percentage. b) Swelling percentage of the polymer films in NaCl solution (0.1M, aqueous) as a function of the EG content. The inset represents the total mass gained by the corresponding polymer films once they uptake hydrated ions and water molecules.

18.References

(1) Vandewal, K.; Goris, L.; Haenen, K.; Geerts, Y.; Manca, J. V. Highly Sensitive Spectroscopic Characterization of Inorganic and Organic Heterojunctions for Solar Cells*. *Eur. Phys. J. Appl. Phys.* **2006**, *36* (3), 281–283.

(2) Ilavsky, J. Nika: Software for Two-Dimensional Data Reduction. *J. Appl. Crystallogr.* **2012**, *45* (2), 324–328.

(3) Oosterhout, S. D.; Savikhin, V.; Zhang, J.; Zhang, Y.; Burgers, M. A.; Marder, S. R.; Bazan, G. C.; Toney, M. F. Mixing Behavior in Small Molecule:Fullerene Organic Photovoltaics. *Chem. Mater.* **2017**, *29* (7), 3062–3069.

(4) Svedhem, S.; Hollander, C.-Å.; Shi, J.; Konradsson, P.; Liedberg, B.; Svensson, S. C. T. Synthesis of a Series of Oligo(ethylene Glycol)-Terminated Alkanethiol Amides Designed to Address Structure and Stability of Biosensing Interfaces. *J. Org. Chem.* **2001**, *66* (13), 4494–4503.

(5) Giovannitti, A.; Nielsen, C. B.; Sbircea, D.-T.; Inal, S.; Donahue, M.; Niazi, M. R.; Hanifi, D. A.; Amassian, A.; Malliaras, G. G.; Rivnay, J.; McCulloch, I. N-Type Organic Electrochemical Transistors with Stability in Water. *Nat. Commun.* **2016**, *7*, 13066.